CARDIOVASCULAR IMAGING

by Bertrand Tavitian

Dear colleagues,

On behalf of the organization committee, it is an immense pleasure to welcome you to the tenth TOPIM Winter School of the European Society for Molecular Imaging on *Cardiovascular Imaging*.

We are particularly happy that the 2016 vintage TOPIM deals with cardiovascular imaging, for two main reasons: **the first reason** is that non-invasive imaging is definitely the method of choice to explore the physiology of the cardiovascular system. It would indeed be highly instructive to write a History of all the erroneous conceptions derived from observations based on invasive techniques — otherwise accurate in many domains of animal biology: from the Egyptian conception of "Ib", the heart, as the organ of conscience and intellect, weighed after our death by Anubis to determine our fate through eternity (Figure 1), from the most respected physiologist Galenus pretending that venous blood carried natural spirit (food) and arterial blood carried vital spirit (heat) (Figure 2), from Hippocrates pretending that arteries carried air, to poor Miguel Servet (Figure 3) burned live in Geneva (not far from Les Houches!) because, according to Calvin, his discovery of pulmonary circulation sacrilegiously raised man to the level of god, science's technical incapacity to observe live the function of the cardiovascular system has hampered its understanding. It was not before the end of the 16th– early 17th century that the term circulation was forged and what it covers correctly described. It may look comforting that non-invasive in vivo imaging easily turns into oblivion all these misconceptions. We must however remain modest: how much of cardiovascular physiology are we still blind to? how many guesses, not to mention wrong statements, do we still make today about e.g. placental circulation, cardiomyocyte metabolism, retrograde signalling at the capillary bed, or even perfusion?

The second reason stems from the first: A new era in cardiac imaging is now showing the heart's function and anatomy by methods that are completely non invasive, in contrast to current catheterization and stress tests. The new technology is based on progress in the science of physics and engineering. Images of each heartbeat are captured by real-time, low radiation dose, multispectral 3D X-ray tomography (CT), made possible by new yttrium-based detectors. Ultrasound signals obtained from molecules submitted to laser pulses uncover the fine structure of arterial walls and drive out atheroma plaques. New fully digital devices replacing photomultipliers improve spatial resolution of PET by a factor of two. Long-awaited hardware and software improvements allow imaging the beating heart with MRI and deciphering cardiac blood flows. Combined PET-MRI opens the hope to perform molecular imaging of coronary accidents. A major trend of progress in imaging is quantification that turns subjective images into objective measurements. All this is happening simultaneously with the development of the implantable artificial heart and accompanying the change in the management and the prognosis of cardiovascular disorders, today's major killer worldwide.

Finally, we are particularly proud that TOPIM has lived through its tenth anniversary, contributing each year a new Hot Topic in Imaging and fertilizing the in vivo imaging science community. This achievement is the result of constant interest and support from the ESMI executive community and of an outstanding level of commitment from the staff of ESMI, in particular from Doris Kracht, as well as constant support from the Ecole de Physique des Houches, its directors and its dedicated staff. Without the enthusiasm and dedication of many, TOPIM would have never lived through its tenth year. In a time where the necessarily questioning of our world by the scientific method is opposed by obscurantism, we must put all our efforts so that TOPIM will remain live and kickin' for many more decades!
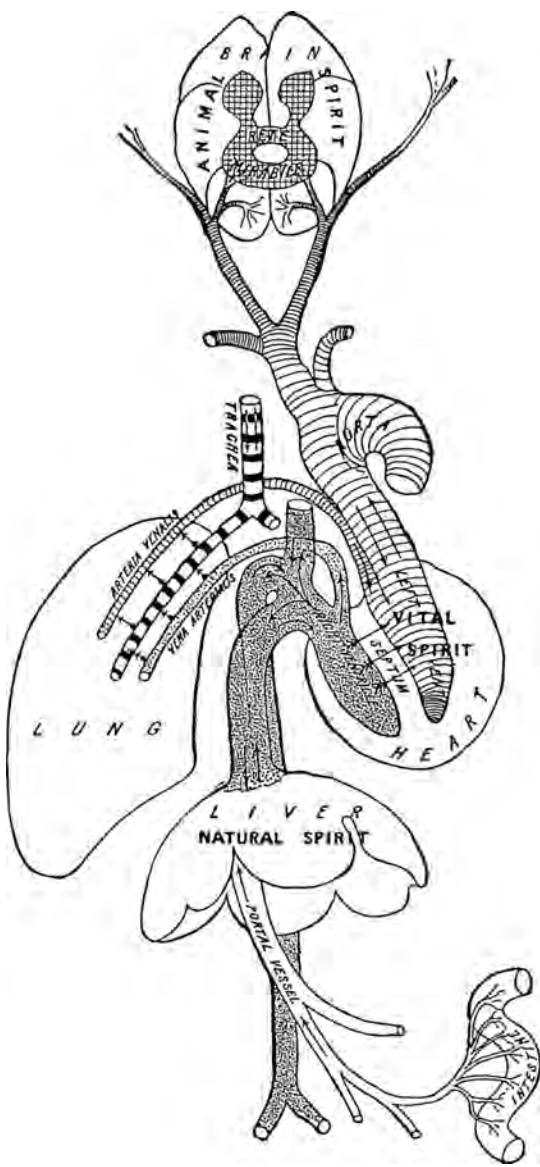
Figure 2: Galen's cardiopulmonary system, which held sway for 1,300 years. During inspiration, pneuma entered the lung through the trachea and reached the left ventricle via the pulmonary vein. Blood was formed in the liver, where it was imbued with natural spirit, and entered the right ventricle. Most then entered the lung but a portion passed through minute channels in the interventricular septum to the left ventricle. Here vital spirit was added and this was distributed through arteries to the rest of the body. The blood that reached the brain was charged with animal spirit that was distributed through the hollow nerves. From John B. West, Galen and the beginnings of Western physiology, Am. J. Physiol. 2014;307(2):L121-8

Figure 1: Anubis, the god with a man's body and a jackal's head, weighing the heart ("Ib") of a deceased opposite an ostrich feather ("Ma'at"). Only hearts lighter than the feather, deemed sinless, would live heavenly after death.

Figure 3: Portrait of Miguel Servet (1511-1553), Spanish doctor of medicine and theology who discovered (or, rather re-discovered some time after the Arab doctor Ibn-al-Afis, 1210-1288), pulmonary circulation.

Bertrand Tavitian

on behalf of the Organization Committte

Michal Neeman - Rehovot

Klaas Nicolay - Eindhoven

Vasilis Ntziachristos - Munich

Michael Schäfers - Münster

welcome   welcome

TOPIM 2016 PROGRAMME OVERVIEW

	Monday 1 February	Tuesday 2 February
07:45 - 08:45		
08:45 - 08:50		
08:50 - 08:55	*Welcome | Bertrand Tavitian*	
08:55 - 09:00		
09:00 - 09:05		Philip Elsinga - Imaging probes for cardiovascular imaging.
09:05 - 09:10		
09:10 - 09:15		
09:15 - 09:20		
09:20 - 09:25		
09:25 - 09:30	**Introductory talk - part I** *Plasticity of the neonatal- and the adult heart.* **Bernd Fleischmann**	
09:30 - 09:35		
09:35 - 09:40		Sven Hermann - Imaging the inflammatory response after myocardial infarction: First results of novel S100A9 specific probes labelled for FRI or SPECT imaging
09:40 - 09:45		
09:45 - 09:50		
09:50 - 09:55		
09:55 - 10:00		Sophie Hernot - Forethought for using Macrophage Mannose Receptor as Target in Atherosclerosis
10:00 - 10:05		
10:05 - 10:10		
10:10 - 10:15		
10:15 - 10:20		
10:20 - 10:25		
10:25 - 10:30		
10:30 - 10:35		
10:35 - 10:40	coffee break	
10:40 - 10:45		
10:45 - 10:50		
10:50 - 10:55		
10:55 - 11:00		
11:00 - 11:05	**Introductory talk - part I** *Plasticity of the neonatal- and the adult heart.* **Bernd Fleischmann**	Stephan Nekolla - Hybrid cardiac imaging with PET/MR: a new kid on the block or here to stay?
11:05 - 11:10		
11:10 - 11:15		
11:15 - 11:20		
11:20 - 11:25		
11:25 - 11:30		
11:30 - 11:35		
11:35 - 11:40		
11:40 - 11:45	**Introductory talk - part II** *Cardiovascular pathophysiologies and clinical challenges for cardiovascular imaging.* **Michael Schäfers**	Vanessa Di Cataldo - What would be the optimal combination of inflammation imaging and tissue analysis for cardiovascular risk assessment? – A study in Non-Human Primates under atherogenic diet
11:45 - 11:50		
11:50 - 11:55		
11:55 - 12:00		
12:00 - 12:05		
12:05 - 12:10		
12:10 - 12:15		
12:15 - 12:20		
12:20 - 12:25		
12:25 - 12:30	*walk to the restaurant*	
12:30 - 13:00	lunch	
13:00 - 16:15	break	
16:15 - 16:20		
16:20 - 16:25		
16:25 - 16:30		
16:30 - 16:35		Frank Bengel - Imaging systems biology in cardiovascular disease.
16:35 - 16:40		
16:40 - 16:45	**Introductory talk - part II** *Cardiovascular pathophysiologies and clinical challenges for cardiovascular imaging.* **Michael Schäfers**	
16:45 - 16:50		
16:50 - 16:55		
16:55 - 17:00		
17:00 - 17:05		Lisa Honold - The extent of monocyte infiltration after myocardial infarction depends on the severity of the ischemic event – a SPECT cell tracking study using HoxB8-Monocytes
17:05 - 17:10		
17:10 - 17:15		
17:15 - 17:20		
17:20 - 17:25		James Thackeray - Imaging of Endogenous Hematopoetic Bone Marrow Cell Trafficking after Myocardial Infarction in Mice using an Inducible Reporter Gene
17:25 - 17:30		
17:30 - 17:35		
17:35 - 17:40	break	
17:40 - 17:45		
17:45 - 17:50		break
17:50 - 17:55		
17:55 - 18:00		
18:00 - 18:05	Adriaan Lammertsma - Measurement of myocardial blood flow and perfusable tissue index.	Philippe Trochet - Multimodality Cardiovascular Imaging: Adding New Dimensions for Functional Assessment of Myocardial Infarction
18:05 - 18:10		
18:10 - 18:15		
18:15 - 18:20		
18:20 - 18:25		
18:25 - 18:30		
18:30 - 18:35		Farouc Jaffer - Intracoronary molecular imaging of atherosclerosis and stents: Movement towards the Cath Lab.
18:35 - 18:40		
18:40 - 18:45	end of the day discussion and expectations	
18:45 - 18:50		
18:50 - 18:55	*walk to the restaurant*	
18:55 - 19:00		
19:00 - 19:05		
19:05 - 19:10	*Welcome drink by the Ecole de Physique*	end of the day discussion
19:10 - 19:15		
19:15 - 19:30		
19:30 (sharp)	dinner	
20:15 - end	come together	come together

TOPIM 2016 PROGRAMME OVERVIEW

	Wednesday 3 February	Thursday 4 February	Friday 5 February
07:45 - 08:45	breakfast		
08:45 - 08:50			
08:50 - 08:55			
08:55 - 09:00			
09:00 - 09:05	Jeanine Prompers - Multimodal imaging of cardiac metabolism in mouse models of heart failure.	Friedemann Kiefer - Approaches to image vascular development and disease in the mouse.	Nico de Jong - Cardiac tissue characterization based on ultrasound imaging of the physics.
09:05 - 09:10			
09:10 - 09:15			
09:15 - 09:20			
09:20 - 09:25			
09:25 - 09:30			
09:30 - 09:35			
09:35 - 09:40	Daniel Balvay - Quantification of arteriogenesis followed by in vivo MR angiography in a rabbit hind limb ischemic model.	Wolfgang Koestner - BLI/CT imaging of IFN-β reporter mice revealed contribution of hepatocytes to IFN-β responses in the liver after Coxsackievirus infection.	Anne Rix - Molecular ultrasound imaging of αvβ3-Integrin in carotid arteries of pigs after vessel injury
09:40 - 09:45			
09:45 - 09:50			
09:50 - 09:55			
09:55 - 10:00	Moritz Wildgruber - Spatially resolved ex-vivo quantification of a gadolinium containing Magnetic Resonance Agent by Matrix-Assisted Laser Desorption Ionization Imaging (MALDI Imaging) – correlation to in-vivo MRI	Cyril Lorentzato - Multimodal nanoparticles functionalized with human antibody fragments designed for Magnetic Particle Imaging of atherosclerosis	Adelina Curaj - Noninvasive Molecular Ultrasound Monit Endothelial Recovery Following Intravascular Surgical Proc Revascularisation
10:00 - 10:05			
10:05 - 10:10			
10:10 - 10:15			
10:15 - 10:20			
10:20 - 10:25			
10:25 - 10:30			
10:30 - 10:35			
10:35 - 10:40	coffee break		
10:40 - 10:45			
10:45 - 10:50			
10:50 - 10:55			
10:55 - 11:00			
11:00 - 11:05	Jessica Bastiaansen - Reporting live and broadcasting in full power: Hyperpolarized MR for metabolic imaging of the heart.	Vasilis Ntziachristos - Optical and Optoacoustic methods for next-generation Cardiovascular Imaging.	best poster presentation II
11:05 - 11:10			
11:10 - 11:15			
11:15 - 11:20			
11:20 - 11:25			
11:25 - 11:30			best poster presentation I
11:30 - 11:35			
11:35 - 11:40			
11:40 - 11:45			
11:45 - 11:50			
11:50 - 11:55	Katrien Vandoorne - MR Mapping of endothelial dysfunction in Cardiac Ischemia	Andrew Heinmiller - High frame-rate photoacoustic imaging of oxygen saturation in the mouse myocardium using ECG-gated kilohertz visualization	*closing remarks*
11:55 - 12:00			
12:00 - 12:05			
12:05 - 12:10			
12:10 - 12:15			
12:15 - 12:20			
12:20 - 12:25			
12:25 - 12:30	*walk to the restaurant*		lunch and departure
12:30 - 13:00	lunch		
13:00 - 16:15	break		
16:15 - 16:20			
16:20 - 16:25			
16:25 - 16:30			
16:30 - 16:35	Reza Razavi - Molecular imaging of cardiovascular disease - is it ready for clinical prime-time?	Klaus Schäfers - The challenge of imaging the moving heart with positron emission tomography: Motion compensation strategies for quantitative data analyses.	
16:35 - 16:40			
16:40 - 16:45			
16:45 - 16:50			
16:50 - 16:55			
16:55 - 17:00			
17:00 - 17:05		Sasha Belenkov - In vivo Quantitative Assessment of Myocardial Structure, Function, Perfusion and Viability using Cardiac Micro-Computed Tomography.	
17:05 - 17:10			
17:10 - 17:15			
17:15 - 17:20			
17:20 - 17:25		Fabian Lohoefer - Assessment and precise quantification of post-infarction scar remodeling using the contrast agent Gadofluorine P and T1 mapping techniques	
17:25 - 17:30			
17:30 - 17:35			
17:35 - 17:40	**poster session** and coffee break		
17:40 - 17:45			
17:45 - 17:50		break	
17:50 - 17:55			
17:55 - 18:00			
18:00 - 18:05		Jereon Essers - Multimodality imaging reveals increased matrix metalloprotease activity and apoptosis preceding cardiac failure in progeroid Ercc1 mice.	
18:05 - 18:10			
18:10 - 18:15			
18:15 - 18:20			
18:20 - 18:25			
18:25 - 18:30			
18:30 - 18:35			
18:35 - 18:40	Moriel Vandsburger - Multi-scale MRI of the heart: molecular methods for cell tracking and tissue characterization.	Michal Neeman - Imaging the role of Akt1 in angiogenesis and cardiovascular disease.	
18:40 - 18:45			
18:45 - 18:50			
18:50 - 18:55			
18:55 - 19:00			
19:00 - 19:05			
19:05 - 19:10	end of the day discussion	end of the day discussion	
19:10 - 19:15			
19:15 - 19:30	*walk to the restaurant*		
19:30 (sharp)		"Savoyard dinner"	
20:15 - end	come together	come together	

TALKS

Monday, 1 February 2016

INTRODUCTORY TALK I

PLASTICITY OF THE NEONATAL- AND THE ADULT HEART

Fleischmann, B.

University of Bonn, Physiology, Sigmund-Freud-Str. 25, 53105 Bonn, Germany

(bernd.fleischmann@uni-bonn.de)

Cardiovascular diseases are the most frequent cause of desath in the western world. In particular large myocardial infarctions and severe heart failure have a poor prognosis, as the only curative approach would be organ transplantation. Because of the shortage of donor organs and the relatively large number of patients affected by these disorders, alternative strategies aimed at enhancing heart function and/or mitigating the most severe complications are warranted.

Our group has a longstanding interest in this topic and therefore analyzes the regenerative potential of the mammalian heart. I will illustrate in my talk different approaches aimed at exploring exogenous- and endogenous repair strategies. These comprise cell replacement and also recent efforts to identify and modulate the cell cycle activity of resident heart muscle cells. I will show that these studies are technically complicated and the results difficult to interpret. We have therefore generated novel animal models in order to enable *ex-* and *in vivo* assessment of cell apoptosis and cell cycle activity in the mammalian heart during development and post-injury. In addition, the need for novel molecular imaging approaches will be documented to better understand extent and mechanisms of the plasticity of the mammalian heart at different time points during development and upon injury. This is particularly important in respect to recent findings that the neonatal heart displays in contrast to the adult stage neo-myogenesis.

The most frequent and potentially severe complications of myocardial infarctions are ventricular arrhythmias and we are currently exploring gene therapy- as well as optogenetic approaches to modulate the electrical activity of the mammalian heart.

A major limitation of current gene therapy and cell replacement approaches are lack of local enrichment and we are therefore probing the use of nanoparticles in combination with custom-made magnets to enhance site specific cell transduction or engraftment of cells.

The present strategies are aimed to improve our mechanistic understanding of cardiac physiology and pathophysiology and to explore experimental therapeutic regimen.

INTRODUCTORY TALK II

CARDIOVASCULAR PATHOPHYSIOLOGIES AND CLINICAL CHALLENGES FOR CARDIOVASCULAR IMAGING

Schäfers, M.

University of Münster Nuclear Medicine, Albert-Schweitzer-Campus 1, 48149 Münster, Germany

(schafmi@uni-muenster.de)

Cardiovascular events most frequently stem from vascular diseases, namely atherosclerosis, with the clinical sequelae myocardial infarction or stroke. These clinical scenarios result from complex inflammatory changes in the vascular wall (atherosclerotic plaques). If these plaques are mechanically unstable ("vulnerable") a rupture or erosion of the plaque surface may eventually lead to thrombosis with partial or complete occlusion of the respective vessel. The organs such as the heart or the brain thus suffer from severe acute ischemia. Despite optimized therapy regimes (Acute PCI, thrombolytic therapies, anti-ischemic medical strategies etc.) a significant loss of cells due to apoptosis and necrosis is observed in many cases with clinical consequences ranging from dysfunction to disability to death.

The incidence of the widespread cardiac disease chronic heart failure resulting from acute or recurrent myocardial infarctions, long-term hypertension, valve diseases or cardiomyopathies is dramatically increasing worldwide. The risk for heart failure approximately doubles with each decade of life. Although the progressive decline in cardiac contractile function is responsible for the majority of deaths due to heart failure, other deadly events might also occur from acute severe tachyarrhythmias. Despite highly potent medical therapies the prognosis of heart failure patients is as poor as for patients with advanced tumor diseases.

The armamentarium of established diagnostic clinical tools together with recently emerging imaging technologies such as magnetic resonance imaging (MRI) allow for a detailed characterisation of the cardiovascular system in men. However, these imaging modalities only provide insight into the morphological and/or functional consequences of cardiovascular diseases and do not assess the underlying pathophysiology of the respective diseases. On the other hand, significant new insight into the molecular basis of cardiovasculardiseases has been gained from genetic screening and the development and application of transgenic animal models.

MEASUREMENT OF MYOCARDIAL BLOOD FLOW AND PERFUSABLE TISSUE INDEX

Lammertsma, A.A..

VU University Medical Center, Department of Radiology & Nuclear Medicine , Amsterdam, The Netherlands

(aa.lammertsma@vumc.nl)

Myocardial blood flow (MBF) in one of the most important parameters in the assessment of myocardial ischaemia, myocardial infarction and other pathological conditions of the heart, with measurements being performed both at baseline and following a pharmacological or physical challenge. Many methods for the measurement of MBF have been proposed, including ultrasound, CT, MRI, SPECT and PET techniques. For quantitative studies, essential for triple vessel disease and for monitoring progression of disease and response to therapy, both high accuracy and high precision are required. It is generally accepted that PET based methods have excellent accuracy and precision.

Three different PET tracers are in common use for the measurement of MBF: 82Rb, 13NH3 and H215O, each with its specific advantages and disadvantages, which will be summarized and discussed. Advantages of H215O are that it is the ideal perfusion tracer (highest accuracy) and that it allows for simultaneous measurements of both MBF and perfusable tissue index (PTI), a measure of tissue viability. In addition, it allows for an intrinsic correction for partial volume and spill-over effects. From a clinical point of view, a major disadvantage has always been the lack of diagnostic parametric MBF images and for many years quantification was performed on a region of interest basis. In the last decade this has changed, partly due to increased sensitivity of state-of-the-art scanners and the number of institutes that use H215O PET for clinical purposes is increasing. In the near future, this development may receive a significant boost as soon as a small (and cheap) H215O dedicated cyclotron becomes available.

In this contribution the principles of measuring myocardial perfusion using PET will be discussed, illustrating the differences between different PET tracers. Next, the tracer kinetic model for measuring MBF and PTI using H215O will be discussed, illustrating how (intrinsic) corrections are introduced for the limited resolution of PET (partial volume effects) and for spill-over from both left and right ventricular cavities. Finally, the various (semi-automatic) steps needed to generate parametric MBF and PTI images will be described.

TALKS
Tuesday, 2 February 2016

IMAGING PROBES FOR CARDIOVASCULAR IMAGING

Elsinga, P. H., Slart, R. H. J. A., Boersma, H.

UMC Groningen Nuclear Medicine and Molecular Imaging, P.O. Box 30001, 9700RB Groningen, Netherlands

(p.h.elsinga@umcg.nl)

The development of imaging probes for cardiovascular imaging is rapidly evolving. Probes become available for PET, SPECT, optical imaging, MRI and hybrid combinations thereof. The imaging probes are used to investigate several targets related to innervation of the heart. With the advent of these imaging probes, sympathetic neurons can be identified by their uptake and storage of false neu-rotransmitters in presynaptic nerve terminals. The uptake of catecholamine analogues is very efficient by presynaptic sympathetic nerve endings, providing high contrast between neuronal and non-neuronal cells. Most of imaging probes allow assessment of the integrity of cardiac innervation, but fail to provide functional parameters quantifying molecular processes such as transport, storage and release of neurotransmitters. More recently, new tracers have been introduced, which display kinetics more suitable for quan-tification of neuronal function. For postsynaptic function many receptor ligands have been developed but their clinical application remains limited so far.

In contrast much effort has been put into imaging of atherosclerosis and vascular targets thereby opening new avenues for cardiovas-cular imaging and corresponding treatment.

This presentation will highlight the current available imaging probes for clinical use including their mode of binding and address novel developments related to imaging probes.

IMAGING THE INFLAMMATORY RESPONSE AFTER MYOCARDIAL INFARCTION: FIRST RESULTS OF NOVEL S100A9 SPECIFIC PROBES LABELLED FOR FRI OR SPECT IMAGING

Hermann, S.[1], Faust, A.[1], Busch, F.[2], Eligehausen, S.[1], Kuhlmann, M.[1], Roth, J.[3], Vogl, T.[3], Schäfers, M.[2,1]

[1]University of Münster European Institute for Molecular Imaging, Waldeyerstrasse 15, 48149 Münster, Germany ; [2]University Hospital Münster Department of Nuclear Medicine, Albert-Schweitzer-Campus 1, Gebäude A1, 48149 Münster, Germany ; [3]University of Münster Institute of Immunology, Röntgenstrasse 21, 48149 Münster, Germany

(shermann@uni-muenster.de)

Introduction: Innate immune cells play a pivotal role in acute inflammatory response and chronic remodelling after myocardial infarc-tion (MI). Activated phagocytes drive the inflammatory activity by releasing high levels of alarmins such as S100A8/S100A9, which are attractive targets for non-invasive molecular imaging. Previously, we successfully showed imaging of inflammatory activity in vivo using the antibody-based probe antiS100A9Cy5.5 (Vogl 2014). Recently, we synthesized the first non-peptidic optical probe (Faust 2015) and together with a novel radiolabelled tracer version, we present here first data of these S100A9 specific tracers in the mouse model of myocardial infarction.

Methods: To characterize the time course of S100A9 presence after MI, we analysed mouse hearts 1d, 3d, 7d, 14d, and 28 days post permanent occlusion of the LAD (n=25) by immunostaining. In vivo evaluation was performed 3d post MI: In the first group (n=8), 3h post i.v. injection of 2nmol of Cy5.5CES271 mice were sacrificed, hearts explanted, cut in halves and FRI was performed employing an en-face technique. In the second group (n=3), whole body SPECT-CT was acquired 5h post i.v. injection of 4 MBq/g body weight of Tc99mFEB054 followed by ex vivo SPECT-CT of the infarcted heart. All imaging experiments were followed by immunohistochemistry.

Results: Histology showed highest S100A9 signals in the infarcted hearts one and 3 days post MI, thereby defining the time window post MI for the imaging studies. FRI of explanted hearts shows increased Cy5.5CES271 signals in the infarcted area with a special emphasis of the borderzone. This distribution pattern is confirmed by FRI of cut hearts and corresponds nicely to immunostaining of S100A9. Furthermore, SPECT-CT of explanted hearts nicely shows accumulation of Tc-99m-FEB054 again in the borderzone of the infarcted area in clear contrast to remote myocardium.

Conclusions: Both, the fluorescent dye labelled and the radiolabelled S100A9-specific tracer accumulate in the S100A9 positive bor-derzone early post MI, thereby visualizing the inflammatory response.

References: Alarmin S100A8/S100A9 as a biomarker for molecular imaging of local inflammatory activity. Vogl et al., Nat Commun. 2014, 5, 4593. Development and evaluation of a non-peptid-ic ligand for the molecular imaging of inflammatory processes using S100A9 (MRP14) as a novel target. Faust et al., Chem. Commun. 2015, 51, 15637.

FORETHOUGHT FOR USING MACROPHAGE MANNOSE RECEPTOR AS TARGET IN ATHEROSCLEROSIS

Bala, G.[1,2], Baudhuin, H.[1], Remory, I.[1,3], Gillis, K.[1,2], Krasniqi, A.[1], Lahoutte, T.[1,4], Devoogdt, N.[1], Droogmans, S.[1,2], Cosyns, B.[1,2], Hernot, S.[1]

[1]Vrije Universiteit Brussel ICMI - BEFY, Laarbeeklaan 103, 1090 Brussels, Belgium ; [2]UZBrussel Cardiology, Laarbeeklaan 101, 1090 Brussels, Belgium ; [3]UZBrussel Anesthestiology, Laarbeeklaan 101, 1090 Brussels, Belgium ; [4]UZBrussel Nuclear Medicine, Laarbeeklaan 101, 1090 Brussels, Belgium

(sophie.hernot@gmail.com)

Introduction: Macrophage accumulation characterizes the development of atherosclerotic plaques. Studies on human tissue demonstrated that the presence of certain macrophage subsets might be an indicator of plaque phenotype and (in)stability. The macrophage mannose receptor (MMR), expressed on alternatively activated macrophages found at sites of intraplaque hemorrhage and neovascularization, has been proposed as target to distinguish vulnerable plaques (1).We aimed to assess the feasibility of using anti-MMR nanobodies (Nbs) (2) as molecular tracers for nuclear imaging in atherosclerosis.

Methods: The anti-MMR Nb (cAbMMR3.49) and control Nb were radiolabeled with ^{99m}Tc using tricarbonyl-chemistry. The radiolabeled Nbs were injected either in ApoE^{-/-} (n=6) or C57Bl/6 mice (n=6). In vivo competition study involving pre-injection of 100-fold excess of unlabeled anti-MMR nanobody (n=3) and injection of anti-MMR Nb in MMR^{-/-} mice (n=3) was performed to demonstrate specificity of the tracer. After SPECT/CT imaging (at 3h p.i.), the mice were sacrificed and radioactive uptake was evaluated in aorta segments. Autoradiography and immunohistochemistry (IHC) staining were performed on aortic sections.

Results: A significant higher uptake was observed in aortic segments of ApoE^{-/-} mice injected with radiolabeled anti-MMR Nb compared to the control nanobody (2.01 ± 0.85 vs 0.26 ± 0.09 %ID/g, p ≤ 0.05). However, a high aortic uptake was also observed in C57Bl/6 mice (1.42 ± 0.47 %ID/g). In vivo competition experiments in these mice showed a significant reduction of the aortic uptake (0.46 ± 0.10 %ID/g, p ≤ 0.05) suggesting a constitutive expression of MMR in healthy aortas. Additionally, the aortic uptake in MMR-KO mice was significantly lower (0.22 ± 0.07 %ID/g, p ≤ 0.05), confirming the specificity of cAbMMR3.49. Autoradiography showed that the localiza-tion of the radioactive signal along the aorta correlated with MMR-expression in perivascular fat tissue as demonstrated by IHC.

Conclusions: No significant uptake of MMR-specific nanobody could be observed in atherosclerotic lesions of ApoE^{-/-} mice. However, the expression of mannose receptor in perivascular fat tissue should be taken into account when trying to image atherosclerotic lesions expressing this target. This could cause for a higher background and thus could be a limitation for the MMR-imaging in vulnerable plaques. Yet, this finding remains to be demonstrated for other animal models and for the human situation.

References: (1) Finn, A.V. et al. Hemoglobin directs macrophage differentiation and prevents foam cell formation in human atherosclerotic plaques. J. Am. Coll. Cardiol. 59, 166–177 (2012). (2) Movahedi, K et al. Nanobody-based targeting of the Macrophage Mannose Receptor for effective in vivo imaging of tumor-associated macrophages. Cancer Res. 72, 4165-4177 (2012).

HYBRID CARDIAC IMAGING WITH PET/MR: A NEW KID ON THE BLOCK OR HERE TO STAY?

Nekolla, S.G.

Nuklearmedizinische Klinik und Poliklinik, Klinikum rechts der Isar der Technischen Universitaet München

(stephan.nekolla@tum.de)

Doubtless, this is primarily a mono-modal imaging world. In the same way as our knowledge of disease in general and cardiac pathology in particular is ever increasing, imaging technology advances every other year or even faster. Still, for the assessment of parameters, which are known to be relevant today, cardiac imaging from every modality has their inherently unique strengths and weaknesses. This basically leads to two distinct scenarios: in the first one, a particular modality tries to emulate the strengths of a "competitor" to derive a valuable parameter – this might come, however, at the price of extended scan time or complex acquisition and processing steps. Or, in an alternative approach, mainly complementary modalities are integrated in hybrid imaging systems which almost by definition increase the costs of investments. Still, in the last decade, SPECT/CT, PET/CT and recently, PET/MR devices were introduced to the cardiac imaging community. This presentation will discuss the advantages and disadvantages of these integrated solutions with respect to effectiveness of workflows, diagnostic accuracies and the synergistic effects. There will be special emphasis on the potential of PET/MR as the range of accessible parameters shows – compared to PET/CT and SPECT/CT – the largest overlap. The combined assessment of not only perfusion but also morpho-functional parameters, molecular information on metabolic and inflammatory processes but also myocardial innervation will improve our understanding of the complex interplay of the highly regulated cardiac system. These integrated devices are an important step towards improved disease understanding and thus implementation of a truly patient centric approach, which facilitates an even tighter integration of the imaging process into the clinical workflow. However, being the system associated with the highest costs, PET/MR needs to show benefits in the setting of more complex diseases centering on altered cardiac metabolism, inflammation and ennervation, where first studies point towards an incremental value.

WHAT WOULD BE THE OPTIMAL COMBINATION OF INFLAMMATION IMAGING AND TISSUE ANALYSIS FOR CARDIOVASCULAR RISK ASSESSMENT? – A STUDY IN NON-HUMAN PRIMATES UNDER ATHEROGENIC DIET

Di Cataldo, V.[1], Piraquive Agudelo, J.[2], Contamin, H.[3], Geloën, A.[1], Grandin, C.[3], Sérusclat, A.[4], Lamberton, F.[2], Ibarolla, D.[2], Lavenne, F.[2], Le Bars, D.[2], Canet-Soulas, E.[1]

[1]INSERM U1060/ INRA 1397 / Lyon 1 University Cardiovascular, Metabolism, diabetes and Nutrition (CarMeN Laboratory), Lyon Sud Faculty of Medicine, 69310 PIERRE-BENITE, France;

[2]CERMEP East Hospital, Boulevard Pinel, 69677 BRON, France ; [3]Cynbiose, VetAgro Sup Campus, 69280 Marcy l'Etoile, France ; [4]Louis Pradel Hospital Departement of radiology, Boulevard Pinel, 69677 BRON, France

(vdicataldo@hotmail.fr)

Introduction: Stratifying the cardio and cerebrovascular risk of atheroma plaques is the greatest difficulty in human clinic. The aim of this study is to work out a stratification tool using blood sampling (lipid profile and inflammation), tissue biological and genomic analysis, and vessel wall inflammation imaging (PET/CT & MRI) in a Non-Human Primate (NHP) model under atherogenic diet.

Methods: Ten 13.1 ±4 years-old Cynomolgus monkeys (3 males and 7ovariectomized females) were fed with atherogenic (23% fat, 0.5% cholesterol) diet (n=13) or standard diet (n=3) during 24 months. Blood sampling was longitudinally performed to assess plasmatic cholesterol, lipoproteins, IL-1β and TNFα level. Characterization of the plaque was performed using ultrasound imaging, PET/CT scan with [18F]FDG and [11C]PK11195 (ligand of TSPO receptor in macrophage mitochondrion). High resolution MRI of the carotids pre and post-Gadolinium was used to analyze vessel wall thickness and gadolinium enhancement. Animals were then sacrified and blood, vessels and tissues of interest removed for further biological and genomic analysis.

Results: At T+18 months, 90% of animals under atherogenic diet displayed lesions at similar location than humans. Atheroma NHPs have a higher cholesterol and inflammation level than controls (p<0.05). Strong correlations between metabolic activity of cells (HK1, GAPDH) and mitochondrion (TSPO), inflammation (IL-1β, TLR4), lymphocyte infiltration (CD3ε) and vulnerable plaque markers (MCP-1, IL-6) were obtained from the genomic analysis. Combining all these data (PET/CT, MRI, biological and genomic markers), NHPs can be divided into 3 groups of cardiovascular risk (low, medium and high) for each vessel of interest.

Conclusions: Using longitudinal lipid and cytokines profile, PET/CT images with [11C]PK11195, MRI and RNA expression, 3 groups of animals were distinguished : low, medium and high cardiovascular risk. This method could be translated to clinical investigations.

References: 1.Register T. Primate models in women's health: inflammation and atherogenesis in female Cynomolgus Macaques. Am J Primatol. 2009: 71(9): 766-775. 2. Shah PK. Biomarkers of plaque instability. Curr Cardiol Rep. 2014: 16: 547-554. 3. Silvera SS, Aidi HE, Rudd JH, et al. Multimodality imaging of atherosclerotic plaque activity and composition using FDG-PET/CT and MRI in carotid and femoral arteries. Atherosclerosis 2009 : 207: 139-43

Figure 2: Genomic study and stratification of cardiovascular risk. (A) Correlation of genes of interest in the carotid arteries. (B) Correlation of genes of interest and PET/CT 18F-FDG uptake (SUV max) in the aortic arch. (C) Stratification of individual cardiovascular risk for aortic cross and carotid arteries.
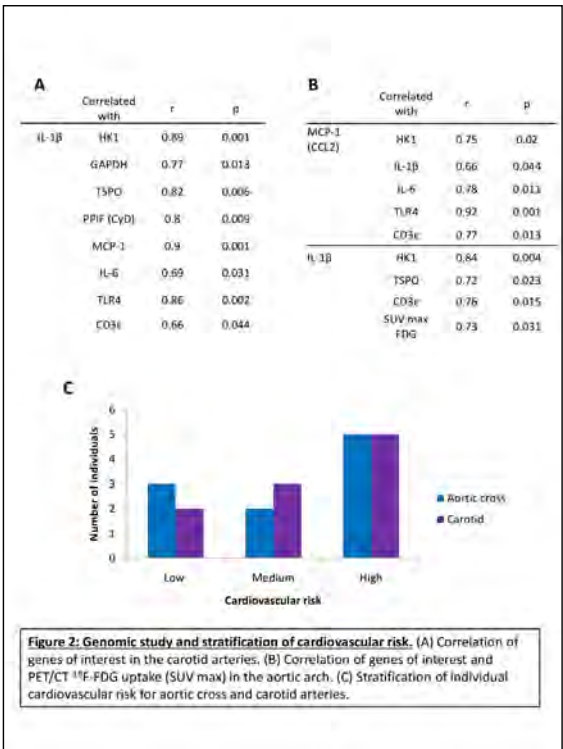
Genomic study: Genomic study and stratification of cardiovascular risk

Figure 1: Imaging modalities for atherosclerosis . (A) CT Angiography and (B) MR Angiography of carotids arteries. (C) 18F-FDG and (D) 11C-PK11195 TEP imaging of carotid arteries with an uptake of both tracers on left carotid (white arrows). (E) 11C-PK11195 TEP imaging showing an uptake on aortic arch (white arrows).
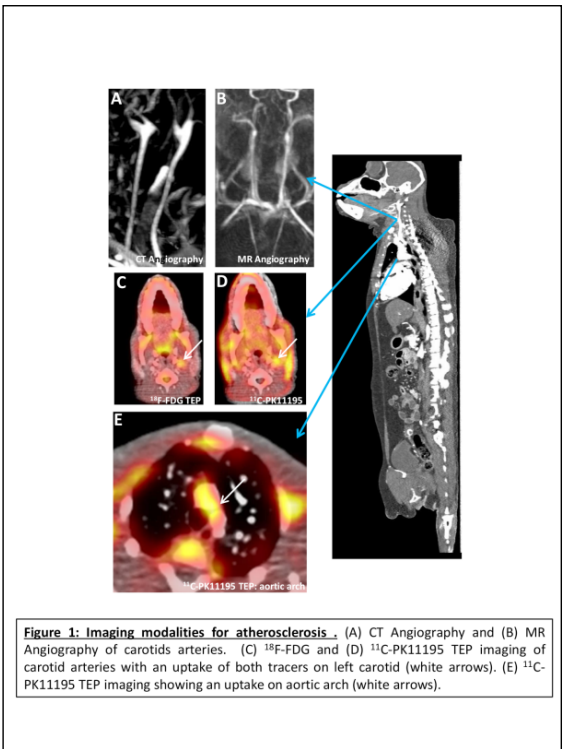
Imaging: Multiple modalities for atherosclerosis imaging

IMAGING SYSTEMS BIOLOGY IN CARDIOVASCULAR DISEASE

Bengel, F. M.

Hannover Medical School Nuclear Medicine, Carl-Neuberg-Str. 1, 30625 Hannover, Germany

(bengel.frank@mh-hannover.de)

The interaction between the heart and extracardiac components of biologic systems is increasingly emphasized in the pathogenesis and progression of cardiovascular disease and in the development and monitoring of novel therapies.

A primary example is the inflammatory hypothesis in atherosclerosis and acute coronary syndromes. Other examples include the role of substrate metabolism in heart failure or the role of the autonomic nervous system in arrhythmia. Likewise, the involvement of the heart in primarily systemic diseases gains increasing attention. Examples are cardiac involvement in sarcoidosis, amyloidosis, and in cancer and cancer therapy.

Owing to the tracer principle and the feasibility of whole-body imaging, molecular imaging is ideally suited to study the impairment of biologic systems, how they affect the heart and vice versa. This has provided novel mechanistic insights and helped to establish innovative therapeutic approaches in cardiovascular medicine.

This lecture will provide several examples and lay a foundation for the hypothesis that imaging may be a key contributor to a paradigm change: Away from a reductionist, organ-focused approach (myocardium, valve, vessels, towards a systems-biology based approach (pathways, cell-cell and organ-organ interaction) in heart disease management.

THE EXTENT OF MONOCYTE INFILTRATION AFTER MYOCARDIAL INFARCTION DEPENDS ON THE SEVERITY OF THE ISCHEMIC EVENT – A SPECT CELL TRACKING STUDY USING HOXB8-MONOCYTES

Honold, L.[1], Gran, S.[2], Eligehausen, S.[1], Hermann, S.[1], Vogl, T.[2], Roth, J.[2], Schäfers, M.[1,3]

[1]University of Muentser European Institute for Molecular Imaging (EIMI), Waldeyerstr. 15, 48149 Münster, Germany ; [2]University of Muenster Institute of Immunology, 48149 Münster, Germany ; [3]University Hospital Muenster Department of Nuclear Medicine, 48159 Münster, Germany

(lisa.honold@wwu.de)

Introduction: Myocardial infarction (MI) is the most common cause of heart failure. In the plethora of post-ischemic events, infiltrating monocytes represent a key factor in infarct healing and tissue remodeling. Non-invasive in vivo imaging methods, such as SPECT, visualizing monocyte infiltration are usually limited by low cell numbers harvested from murine tissue. In contrast, HoxB8-immortalized myeloid progenitor cells differentiated into monocytes and labeled in vitro provide a unique platform to overcome these limitations. Here, we compared the extent of monocyte infiltration after permanent infarction and transient myocardial ischemia, using a radioactive and fluorescent dual-labeling approach.

Methods: HoxB8-Monocyte progenitors were differentiated into monocytes for 3 days and subsequently dual-labeled with ^{111}In-Oxine and VivoTrack680. C57Bl6 mice underwent surgery for either permanent or transient (60min) ligation of the LAD coronary artery. The ischemic area at risk was assessed immediately after surgery by ^{99m}Tc-Tetrofosmin perfusion SPECT. 1 day post surgery 10*10[6] labeled HoxB8-Monocytes were injected into the tail vein and SPECT/CT scans acquired 24h and 48h p.i.. Following the last acquisition, mice were sacrificed and the biodistribution of injected monocytes assessed via FRI, autoradiography and dedicated histology.

Results: In the model of permanent ischemia (PI), migrated HoxB8-Monocytes are detectable 24 and 48h p.i. by SPECT imaging as shown by significantly increased infarct/remote SUV ratios (I/R d1: 1.62±0.3, p=0.02; d2: 1.98±0.7, p=0.01; n=5), whereas uptake into the area of infarction in transient ischemia (TI) is only significantly increased on day 2 (I/R d1: 1.47±0.6, p=0.39; d2: 1.67±0.3, p=0.03; n=3) (Fig.1b).

Ex vivo optical imaging confirms increased migration of monocytes in PI compared to TI (Rad.efficiency (x10^{8}) PI: 3.57±0.6 vs TI: 1.14±0.3; p<0.01) (Fig.1c). The amount of migrated cells as determined by FRI correlates with the ischemic area at risk. Autoradiography and histology confirm the localization of labeled cells in the infarcted myocardium.

Conclusions: HoxB8-Monocytes provide a unique system to non-invasively study monocyte migration and infiltration after myocardial infarction. The combination of nuclear and optical imaging provides a powerful platform to visualize the extent of monocytes migrating into the area of ischemia. We report that the magnitude of monocyte infiltration depends on the type of ischemic event, with more cells infiltrating in our model of permanent infarction compared to transient myocardial ischemia. We are currently investigating the effect of increased ischemia intervals on monocyte recruitment in transient ischemia.
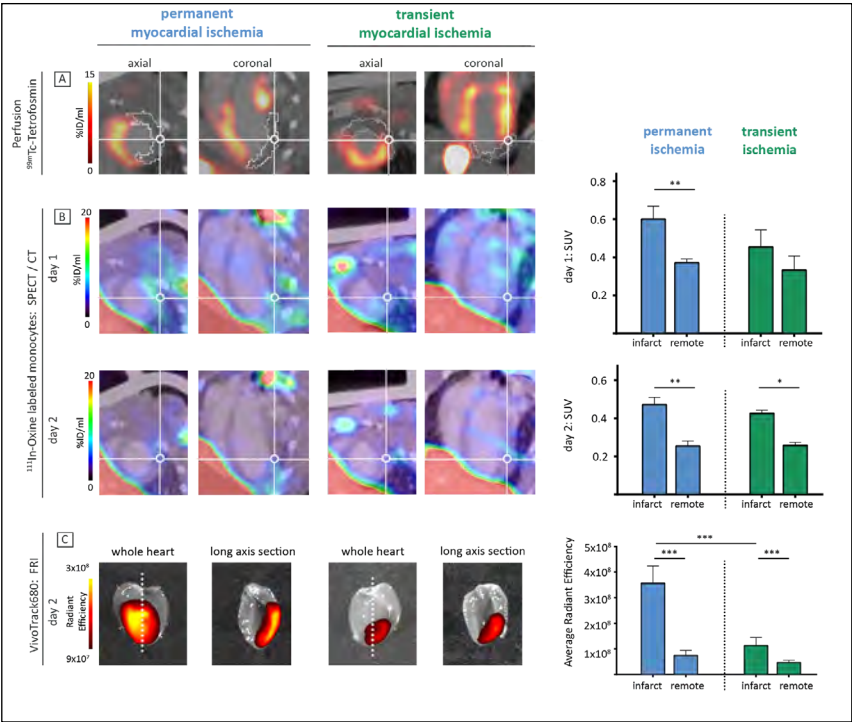
Figure 1: HoxB8-Monocytes dual-labeled with 111In-Oxine and VivoTrack680 migrate into the area at risk, with increased monocyte infiltration in permanent compared to transient ischemia
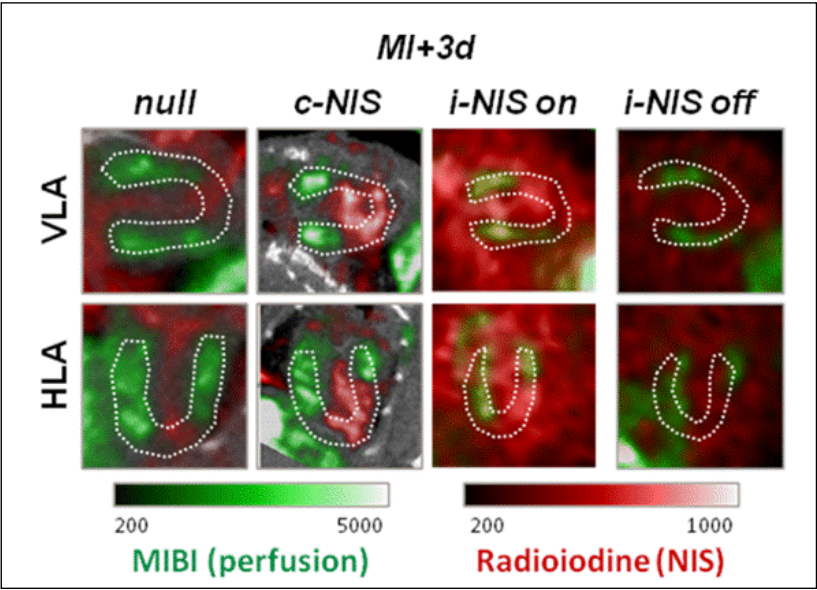

Figure.: Dual isotope SPECT imaging demonstrates selective accumulation of radioiodine by NIS-expressing cells within the perfusion defect at 3d after coronary artery occlusion

IMAGING OF ENDOGENOUS HEMATOPOETIC BONE MARROW CELL TRAFFICKING AFTER MYOCARDIAL INFARCTION IN MICE USING AN INDUCIBLE REPORTER GENE

Thackeray, J. T.[1], Korf-klingebiel, M.[2], Wang, Y.[2], Kustikova, O. S.[3], Bankstahl, J. P.[1], Wollert, K. C.[2], Bengel, F. M.[1]

[1]Hannover Medical School Department of Nuclear Medicine, Carl Neuberg Str 1, 30625 Hannover, Germany ; [2]Hannover Medical School Department of Cardiology and Angiology, Carl neuberg Str 1, 30625 Hannover, Germany ; [3]Hannover Medical School Department of Experimental Haematology, Carl Neuberg Str 1, 30625 Hannover, Germany

(Thackeray.James@mh-hannover.de)

Introduction: The limited clinical benefit described for exogenous stem cell therapy has fortified the design of therapies to support endogenous cell recruitment after myocardial infarction (MI). Imaging studies with labeled stem cells have been restricted to exogenous cell transplantation, and are hampered by low cell retention and permanent potentially detrimental expression of reporter genes. We investigated the feasibility of bone marrow transplant with hematopoetic stem cells (HSCs) conditionally expressing sodium iodide symporter (NIS) reporter gene for imaging of bone marrow repopulation and endogenous cell trafficking after MI.

Methods: NIS was cloned into a lentiviral vector under a constitutive (c-NIS) or doycycline-inducible promoter. HSCs were transduced with c-NIS, i-NIS, or null lentivirus. C57Bl/6 mice (n=57) were lethally irradiated and transplanted with HSCs tranduced with either c-NIS, i-NIS, or null lentivirus (5x10⁵). Coronary artery ligation was performed at 6-8 weeks after transplant. Doxycycline (dox) was provided to subgroup of i-NIS mice 4d prior to MI.

Results: Serial SPECT imaging demonstrated higher radioiodine uptake localized to the perfusion defect in c-NIS compared to NIS-null transplanted mice (TBR infarct: MI+3d, 3.0±0.3 v 1.6±0.1 p<0.001; MI+7d, 3.1±0.9 v 1.4±0.3 p<0.01). A comparable increase was observed in i-NIS transplanted mice. The relative uptake in the infarct territory compared to the remote was higher in c-NIS versus NIS null transplanted mice (+6.5±0.2%, p<0.05). i-NIS transplanted mice treated with dox exhibited higher radioiodine signal in whole myocardium compared to untreated at 1d post-MI (TBR: 2.0±0.3 v 1.6±0.3, p=0.04), but not at 7d post-MI (TBR: 1.5±0.5 v 1.3±0.1, p=0.27). Ex vivo biodistribution and multi-isotope autoradiography confirmed the presence of radioiodine within the infarct wall, which was further associated with histological indicators of inflammation.

Conclusions: Bone marrow transplant with NIS reporter gene-labeled HSCs enabled imaging of endogenous cell trafficking after MI. The conditional construct may prove beneficial for intricately timed and targeted delivery and/or monitoring of therapeutic agents.

MULTIMODALITY CARDIOVASCULAR IMAGING: ADDING NEW DIMENSIONS FOR FUNCTIONAL ASSESSMENT OF MYOCARDIAL INFARCTION

Jose, J., Fuchs, D., Heinmiller, A., Forbrich, A., Trochet, P.

FUJIFILM VisualSonics, Joop Geesinkweg 140, 1114AB Amsterdam, Netherlands

(ptrochet@visualsonics.com)

Introduction: Visualizing the myocardium anatomy and assessing cardiac function are important in diagnosing cardiovascular diseases (CVD). Real-time and non-invasive imaging modalities are essential to provide functional and molecular information together with the anatomical details. Here we present a multimodal approach to image the cardiac function and assess the functional and molecular information based on a combined photoacoustic (PA) and High-resolution Ultrasound Imaging.

Methods: Imaging was performed on the Vevo® LAZR system (FUJIFILM VisualSonics) at 18-38 MHz. The system features hybrid ultrasound transducer with photoacoustic capabilities providing an axial resolution of 50 um. Murine healthy and myocardial infarct models were imaged. The experiments were approved by the local ethical committee. Cardiac function and speckle tracking based wall motion were assessed by taking long and short axis views and compared between healthy and diseased mice. Myocardial oxygenation levels were obtained by using photoacoustic oxygenation imaging [1].

Results: Values for fractional shortening, stroke volume, and cardiac output were used as a measure for cardiac function. Regional speckle tracking was used to evaluate changes in myocardial strain and strain rate. Photoacoustic images obtained at 820 nm showed the anterior myocardium throughout multiple cardiac cycles. Interventricular spectrum walls, right atrium and the apex were clearly visible in the single wavelength image. PA oxygenation imaging was also performed and the obtained results of oxygenation showed a clear difference between the healthy and diseased models. The addition of PA oxygenation measurements together with the cardiac functional imaging increases the sensitivity of detecting CVD.

Conclusions: In the present work we have demonstrated the multi-modal capabilities of high resolution ultrasound and photoacoustic imaging. We show the first a true "full cardiac exam" covering systolic and diastolic function, strain analysis as well as myocardium oxygenation levels using one imaging device, thus adding a new dimension for cardiovascular diagnosis.

References: Needles et al., "Development and initial application of a fully integrated photoacoustic micro-ultrasound system," IEEE Trans Ultrason Ferroelectr Freq Control 60(5), 888-897 (2013).

INTRACORONARY MOLECULAR IMAGING OF ATHEROSCLEROSIS AND STENTS:
MOVEMENT TOWARDS THE CATH LAB

Jaffer, F.

Cardiovascular Research Center, Cardiology Division, Massachusetts General Hospital, Harvard Medical School

(fjaffer@mgh.harvard.edu)

Progression of vulnerable coronary atherosclerotic plaques underlie the majority of acute myocardial infarction and sudden cardiac death episodes. Recent advances in biological and molecular imaging technology may now provide accurate identification of high-risk plaques and high-risk stents. Due to their small size and cardiorespiratory motion, noninvasive molecular imaging approaches remain challenging for application to human coronary artery disease. Therefore, intravascular molecular imaging approaches are likely necessary to resolve molecular details at sufficient resolution for human coronary arteries. Here we present recent progress in intravascular near-infrared fluorescence (NIRF) molecular imaging, including the evolution from standalone NIRF systems to those integrated with structural imaging methods such as optical coherence tomography or intravascular ultrasound. Preclinical demonstrations of imaging inflammation, fibrin, and endothelial impairment are showcased. We then close with a discussion of translation of NIRF imaging to the cardiac catheterization laboratory and discuss first-in-human intracoronary imaging results of NIR autofluorescence in CAD.

TALKS
Wednesday, 3 February 2016

MULTIMODAL IMAGING OF CARDIAC METABOLISM IN MOUSE MODELS OF HEART FAILURE

Abdurrachim, D.[1], Nabben, M.[1,2], Hoerr, V.[3,4], Kuhlmann, M.[5], Bovenkamp, P.[3], Schäfers, M.[5], Nicolay, K.[1], Faber, C.[3], Hermann, S.[5], Prompers, J.[1]

[1]Eindhoven University of Technology Biomedical NMR, Department of Biomedical Engineering, Eindhoven, Netherlands; [2]Maastricht University Department of Genetics and Cell Biology, Cardiovascular Research Institute Maastricht (CARIM), Maastricht, Netherlands; [3]University Hospital Münster Department of Clinical Radiology, Münster, Germany ; [4]Jena University Hospital Institute of Medical Microbiology, Jena, Germany ; [5]European Institute for Molecular Imaging-EIMI, Münster, Germany

(j.j.prompers@tue.nl)

Background: Heart failure has been associated with altered myocardial substrate metabolism and impaired cardiac energetics. However, it is currently not clear whether these alterations are cause or consequence of heart failure progression. Furthermore, comorbidities such as diabetes may influence the metabolic adaptations during heart failure. In this study, we aim to quantify the cardiac metabolic changes during different stages of heart failure progression in non-diabetic and diabetic mice in a longitudinal *in vivo* study design.

Methods: Transverse aortic constriction (TAC) surgery was performed in non-diabetic db/+ and diabetic db/db mice to induce pressure overload heart failure. Magnetic resonance imaging (MRI), ^{31}P magnetic resonance spectroscopy (MRS), ^{1}H MRS, and ^{18}F-fluorode-oxyglucose-positron emission tomography (^{18}F-FDG-PET) were applied to measure cardiac function, energy status, lipid content, and glucose uptake (Figure 1), respectively, at baseline and 1, 5, and 12 weeks post TAC.

Results: In non-diabetic mice, TAC induced progressive left ventricular (LV) hypertrophy and dysfunction, which correlated with myocardial FDG uptake. Myocardial FDG uptake was increased at 1 and 5 weeks post TAC, but tended to decrease again at 12 weeks post TAC, which was associated with a trend for lowered cardiac energy status. Interestingly, whereas diabetic mice showed overall lower myocardial FDG uptake, lower cardiac energy status, and higher myocardial lipid accumulation than non-diabetic mice at baseline, the effects of TAC on LV mass and function were much less prominent than in non-diabetic mice. Also in diabetic mice, myocardial FDG uptake increased upon TAC, but it remained lower than in non-diabetic mice. Myocardial lipid content and cardiac energy status in diabetic mice were not affected by TAC.

Conclusion: This study presents the first longitudinal *in vivo* data of cardiac metabolic and functional adaptations during heart failure development in non-diabetic and diabetic mice. The mild cardiac hypertrophy and dysfunction in diabetic mice, together with lower myocardial glucose uptake upon TAC, suggests that maintaining fatty acid oxidation may be beneficial for cardiac function and energetics in pressure overload-induced heart failure. Non-invasive multimodal imaging provides a comprehensive view of changes in cardiac metabolic adaptations during different stages of the development and progression of heart failure, which is crucial for our understanding of the pathophysiology and the design of more effective strategies to treat heart failure.
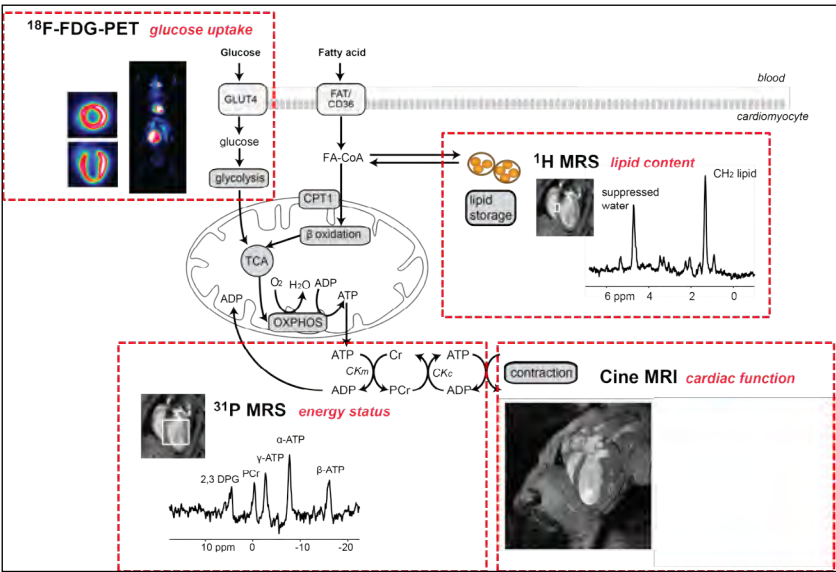

Figure 1: Non-invasive imaging techniques for the measurement of in vivo cardiac metabolism and function

QUANTIFICATION OF ARTERIOGENESIS FOLLOWED BY *IN VIVO* MR ANGIOGRAPHY IN A RABBIT HIND LIMB ISCHEMIC MODEL.

Casanova, A.[1], Marijon, C.[1], Balvay, D.[1,2], Autret, G.[1,2], Bellamy, V.[1], Larghero, J.[3], Vanneaux, V.[3], Menasché, P.[1,4], Clément, O.[1,5]

[1]INSERM / Université Paris Descartes, Sorbonne Paris Cité Paris Cardiovascular Research Center, UMR_970, 56 rue Leblanc, 75015 Paris, France ; [2]Université Paris Descartes, Sorbonne Paris Cité Plateforme Imageries du Vivant, 56 rue Leblanc, 75015 Paris, France ; [3]Assistance Publique - Hôpitaux de Paris, Hôpital St Louis Departement of cell therapy, 1 Avenue Claude Vellefaux, 75010 Paris, France ; [4]Assistance Publique - Hôpitaux de Paris, Hôpital Européen Georges Pompidou Departement of cardiovascular surgery, 20 rue Leblanc, 75015 Paris, France ; [5]Assistance Publique - Hôpitaux de Paris, Hôpital Européen Georges Pompidou Departement of radiology, 20 rue Leblanc, 75015 Paris, France

(daniel.balvay@inserm.fr)

Introduction: The aim of this study was to propose a supervised method based on MR angiography (MRA), for the evaluation of the collateral development (arteriogenesis) in hind limb ischemic model, as an alternative to the most current post mortem angiogram analysis.

Methods: Twenty rabbits, selected from a cell therapy study, underwent a unilateral total resection of femoral artery. Axial MR (Time of Fly) Angiography sequences were performed at D2, D17 and D35 post-surgery, on a 4.7T small animal MRI. A 3D segmentation software was developed to measure vascular volumes in ischemic and contralateral limbs. It included vascular segmentation (k-means; user correction), ischemic / contralateral region setting (upper delineation; 3D segment by segment correction), large vessel exclusion (morphologic filtering), and a data management system. Ischemic and controtrolateral were compared for each time points and differences were evaluated statistically by using the signed Wilcoxon test.

Results: Roughly, vascular volumes were obtained in 5 minutes per exam (Fig. 1), then they were collected (Fig. 2). For moderate caliber, a clear arteriogenesis was demonstrated in the ischemic side (p = 0.013, p <0.001, p <0.001 resp. for D2, D17 and D35). Moreover, in line with literature [1], a difference in arteriogenesis between the acute (D2) and the sub-acute phases (D17, D35) was observed: p=0.012, p=0.002 resp. Rationally, no results were found for large vessels affected by surgery.

Conclusions: Our results demonstrated the consistence of MRI to follow collateralization in rabbit hind limb ischemic model. MRA should provide in vivo information completing post mortem information as angiograms and histology which are more focused in biomechanical and architectural observations.

References: Hoefer IE, van Royen N, Buschmann IR, Piek JJ, Schaper W. **Time course of arteriogenesis following femoral artery occlusion in the rabbit.** Cardiovasc Res. 2001 Feb 16;49(3):609-17.
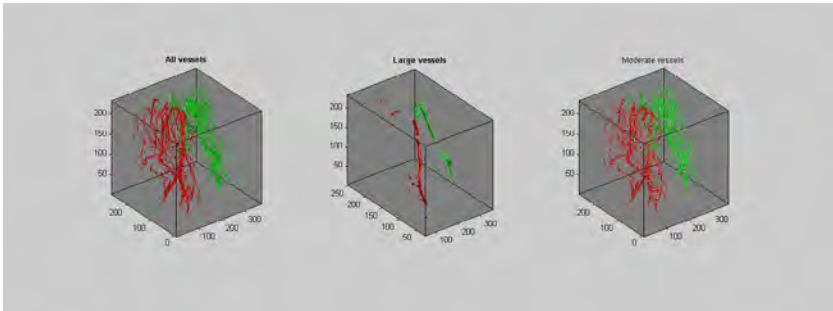
Figure 1: Example of a vascular segmentation, before and after large vessel removing. In red: ischemic side; in green: contralateral side. Left: all vessels; Center: large vessels; Right: moderate vessels.
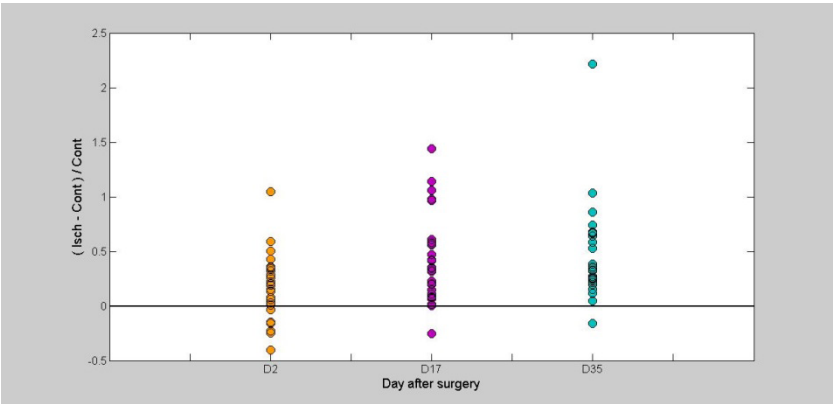
Figure 2: Collateralization compensation in the ischemic thigh in acute and sub-acute phases. Most of exams indicated an increase of vascularization of large vessel in the ischemic thigh compared to the control thigh (means: D2: + 18%; D17 : +42%; D35 : +46%).

SPATIALLY RESOLVED EX-VIVO QUANTIFICATION OF A GADOLINIUM CONTAINING MAGNETIC RESONANCE AGENT BY MATRIX-ASSISTED LASER DESORPTION IONIZATION IMAGING (MALDI IMAGING) – CORRELATION TO IN-VIVO MRI

Wildgruber, M.[1], Aichler, M.[2], Huber, K.[2], Lohöfer, F.[1], Walch, A. - K.[2]

[1]Technische Universität München Department of Radiology, Ismaningerstrasse 22, 81675 München, Germany ; [2]Helmholtz Zentrum München Research Unit Analytical Pathology, Neuherberg, Germany

(moritz.wildgruber@tum.de)

Introduction: Analysis of magnetic resonance contrast agents in tissue sections has remained a challenge so far. Our purpose was to evaluate MALDI Imaging for spatially resolved ex-vivo quantification of a gadolinium-based Magnetic Resonance Agent in correlation to in-vivo Magnetic Resonance Imaging.

Methods: In-vivo deposition of Gadofluorine M was investigated in a mouse model of myocardial infarction. Mice were investigated by in-vivo MRI at 7T at 6h, 24h and 48h after injection of 0.2mmol/kg Gadofluorine M. Delayed enhancement was detected in the infarct scar using a conventional FLASH technique and quantified by calculating signal- and contrast-to-noise ratios. Additionally T1 mapping studies were performed using a snapshot technique. Animals were sacrificed after each time point and hearts were prepared for quantitative assessment by MALDI Imaging.

Results: Delayed enhancement imaging revealed signal enhancement in the myocardial scar beginning at 6h after Gadofluorine M injection with peak enhancement at 24h hours and residual enhancement at 48h post injection. Contrast-to-noise ratios were highest at 24h post injection due to high agent accumulation in the infarct and low signal from the blood. T1 values in the infarct were shortest at 6h and steadily increased to 24h and 48h post injection. MALDI Imaging was able to corroborate the in-vivo imaging results and enabled in-situ quantification of the in-vivo applied Gadolfuorine M with high spatial resolution.

Conclusions: MALDI Imaging is able to provide a mass-specrometry based quantification of gadolinium containing contrast agents in situ with high spatial resolution. The results of MALDI Imaging correlate with in-vivo MRI. For the first time quantitative ex-vivo validation of in-vivo contrast agent distribution is possible.

References: Aichler M, Huber K, Schilling F, Lohöfer F, Kosanke K, Meier R, Rummeny EJ, Walch AK, Wildgruber M (2015). Spatially Resolved Quantification of Gd (III)-based Magnetic Resonance Agents in Tissue by MALDI Imaging Mass Spectrometry after *in vivo* MRI. Angew Chem Int Ed Engl; 54:1-6
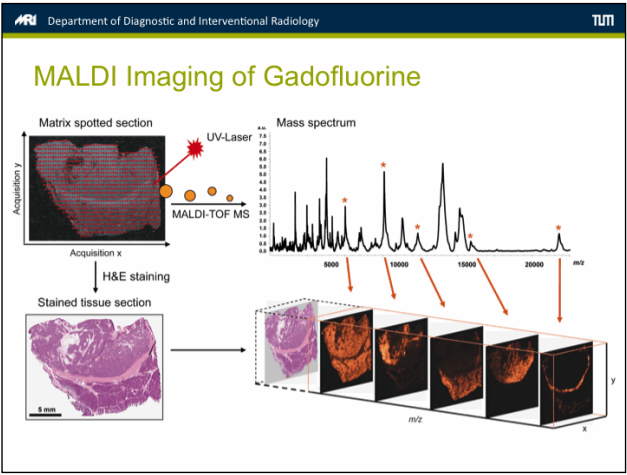
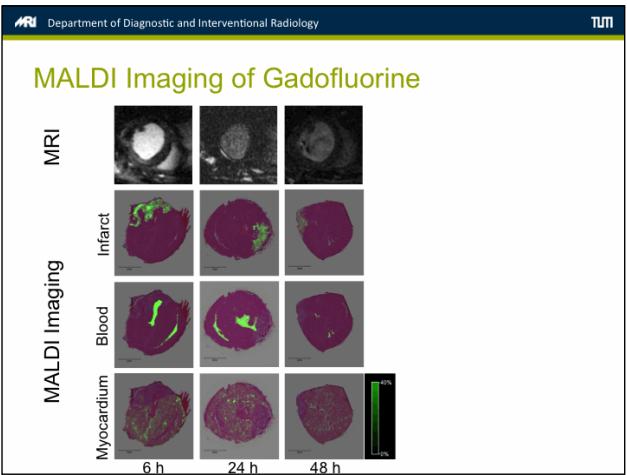Figure 1: Principle of MALDI Imaging

Figure 2: MALDI Imaging of Gadofluorine

REPORTING LIVE AND BROADCASTING IN FULL POWER: HYPERPOLARIZED MR FOR METABOLIC IMAGING OF THE HEART

Bastiaansen, J.[1,2]

[1]University Hospital Lausanne (CHUV) Department of Radiology, Rue de Bugnon 46, 1011 Lausanne, Switzerland; [2]Swiss Federal Institute of Technology Institute of Physics of Biological Systems, Lausanne, Switzerland

(jbastiaansen.mri@gmail.com)

Cardiac muscle function depends on a continuous energy production, with a fine balance between substrate delivery and utilization. Myocardial dysfunction and disease progression are often linked with changes in substrate metabolism, alterations in myocardial Krebs cycle turnover and ATP production. In fact, metabolic changes are increasingly being identified as playing intrinsic roles in many diseases. Understanding the biochemical mechanisms underlying pathologies requires the ability to investigate metabolic processes in vivo.

Magnetic resonance (MR) can provide insight on biological processes using spectroscopic techniques such as carbon-13 MR spectroscopy (^{13}C MRS). However, the low concentration of carbon-containing molecules, combined with the low natural abundance and sensitivity of the ^{13}C nucleus, makes this type of measurement challenging. Hyperpolarized MR technology addresses the sensitivity issue of ^{13}C MRS, with signal enhancements over 10,000 fold using dissolution dynamic nuclear polarization (dDNP). This promising technology enables the "live" measurement of ^{13}C labeled metabolites and their downstream metabolic products within seconds after injection. Due to its high sensitivity and specificity, dDNP has the unique ability to detect and quantify real-time metabolic changes in vivo. Furthermore, the combination of hyperpolarized ^{13}C MRS and co-administration of separate imaging agents allow the measurement of dual substrate metabolism: Simultaneous monitoring of both fatty acid and carbohydrate metabolism *in vivo* in a single experiment.

For the clinical translation of dDNP, which uses ^{13}C preparations containing free radicals, a time consuming filtration process is necessary before injection. This, combined with additional pharmaceutical quality control tests on the solution, results in losses of polarization, and thereby of sensitivity. Novel developments using UV irradiation of the ^{13}C substrates has shown that radical-free preparations and injections of hyperpolarized pyruvic acid are possible, and these techniques can be extended to mixtures of ^{13}C labeled metabolites.

Radical-free co-hyperpolarization of multiple ^{13}C-labeled metabolites enables noninvasive and simultaneous monitoring of separate metabolic pathways in a single experiment. In addition, the removal of the need for filtering out free radicals could shorten the time from dissolution to injection, increasing the sensitivity, and promising a method for measuring multiple substrate metabolism that could be translated to humans.

In this overview, the principles, state of the art, and emerging methods for hyperpolarized MRS in the heart will be presented and discussed

MR MAPPING OF ENDOTHELIAL DYSFUNCTION IN CARDIAC ISCHEMIA

Vandoorne, K.[1], Vandsburger, M. H.[2], Jacobs, I.[1], Han, Y.[1], Dafni, H.[3], Nicolay, K.[1], Strijkers, G. J.[1,4]

[1]Eindhoven University of Technology Biomedical NMR, Department of Biomedical Engineering, HTC 11, AE5656 Eindhoven, Netherlands; [2]University of Kentucky Department of Physiology, Lexington, Kentucky United States; [3]Weizmann Insitute of Science Department of Veterinary Resources, 72600 Rehovot, Israel ; [4]Academic Medical Center Department of Biomedical Engineering and Physics, Amsterdam, Netherlands

(k.vandoorne@tue.nl)

Introduction: Mouse imaging studies play a crucial role in understanding the dynamics of ischemic cardiac disease. However, non-invasive preclinical methods to characterize myocardial vascular function are still lacking. Ischemic heart disease is associated with myocardial endothelial dysfunction resulting in leakage of plasma albumin into the extravascular space. As we demonstrate here, these features can be harnessed in a noninvasive three-dimensional MR imaging method to measure fractional blood volume (fBV) and vascular permeability (PS) using labeled albumin as a blood pool contrast agent.

Methods: C57BL/6 mice were imaged before (n=6) and 3 days (n=7) after surgically induced myocardial infarction (MI). Late gadolinium enhanced (LGE) MRI using Gd-DTPA was performed one day after MI to verify similar infarct sizes (Fig.1a). Measurements were performed on a 9.4T Bruker scanner using a 72-mm volume coil with a 4-channel phased-array coil (Bruker Biospin, Ettlingen Germany). Three-dimensional (3D) Intragate FLASH images of the entire heart with retrospective gating were acquired before and after intravenous injection of macromolecular albumin-Gd-DTPA (10mg/mouse in 200ml; Relaxivity r_1=130mM^{-1}s^{-1}; SyMO-Chem, Eindhoven, The Netherlands). Following quantitative T_1-mapping, dynamics of intravenously injected albumin-based contrast agent, extravasating from permeable (dysfunctional) myocardial blood vessels, were tracked on short-axis MR images of the entire heart. Maps of fractional blood volume (fBV) and permeability surface area product (Permeability) were calculated in MATLAB (Mathworks, Natick, MA, USA). Red fluorescent rhodamine covalently bound to the albumin-based contrast agent was used to validate the MR finding by ex vivo fluorescence microscopy.

Results: This study successfully discriminated between infarcted and peri-infarcted regions three days post-infarct, based on a reduced fractional blood volume (fBV; Fig 1b, c, f)) in the infarcted region and increased permeability surface area product (PS; Fig 1d, e, g) in the infarcted and peri-infarcted regions. These findings were confirmed using *ex-vivo* fluorescence imaging and histology (Fig 1h, i).

Conclusions: We have demonstrated the quantification of blood volume and permeability in the infarcted myocardium, providing an imaging biomarker for assessment of myocardial endothelial dysfunction. The presented method has the potential to track endothelial function for longitudinal cardiac studies determining pathophysiological processes and disease progression during infarct healing.
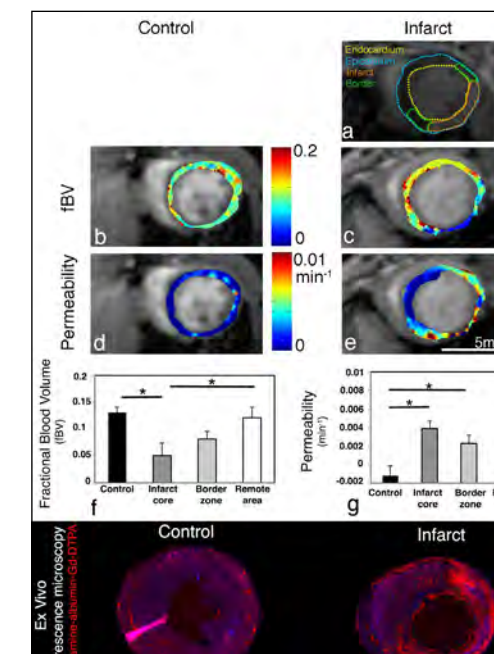

Figure 1: (a) LGE images 1 day after MI. Representative midventricular cardiac MR images in gray with in color (b,c) fBV and (d,e) permeability maps of the myocardium. Values for (f) fBV and (g) permeability. (h,i) Ex vivo fluorescence microscopy of myocardium

## MOLECULAR IMAGING OF CARDIOVASCULAR DISEASE – IS IT READY FOR CLINICAL PRIME-TIME?

Razavi, R.

Imaging Sciences and Biomedical Engineering, King's College London, UK

(reza.razavi@kcl.ac.uk)

Heart and circulatory diseases cause 40% of deaths and disabilities worldwide. Atherosclerosis involves the thickening of the vessel wall that obstructs blood flow to the downstream tissue. If the artery is in the coronary tree lack of blood flow will cause a myocardial infarction whereas if the plaque is situated in the carotid artery it will cause a stroke. Atherosclerosis is a complex disease that involves several biological processes that are summarized on this diagram.
Several target MRI-based contrast agents have been developed to elucidate and investigate different aspects of disease progression.
There are 3 major pathways to transport compounds/molecules across the vascular endothelium.
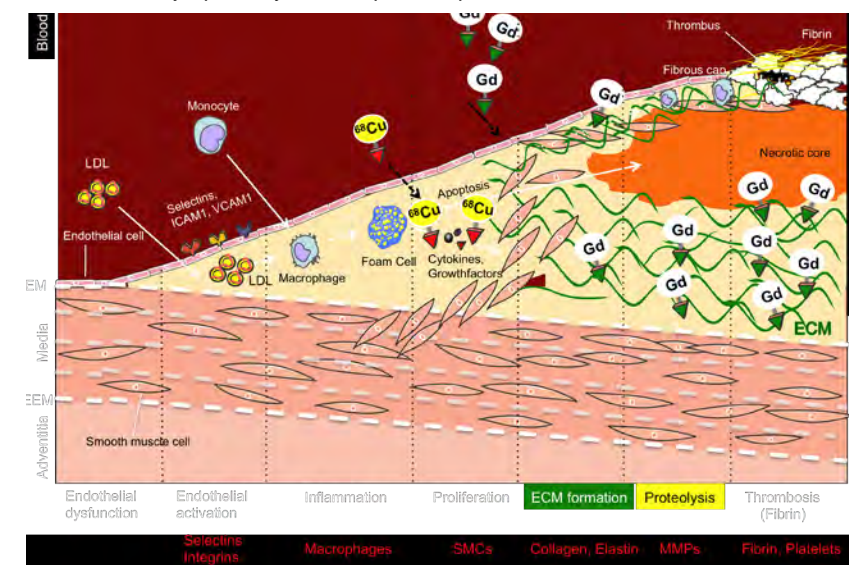
- Trans: where molecules bind to cell-surface receptors/ become engulfed in vesicles and then internalized
- Paracellular: through normally existing "breaks" in the junctions that allow transport of some molecules
- Between leaky tight junctions that are > that 20nm wide and exist between apoptotic, dividing endothelial cells.
One way to measure vascular permeability is by the use of albumin-binding dyes. Vasovist or Gadofosveset is a Gadolinium contrast agent which binds to albumin and therefore can be used for permeability studies in the vessel wall.

Recently, colleagues at King's used the albumin-binding contrast agent – Gadofosveset to assess endothelial permeability in a murine model. Using this approach they were able to monitor & quantify plaque progression in the brachocephalic artery of atherosclerotic ApoE mice. Interestingly, the uptake of the contrast agent was regionally and quantitatively similar to that of EBD, an established histological technique used in permeability studies.

Functionally, the endothelial cells in the presence of atherosclerosis showed impaired vasodilation/paradoxical vasoconstriction in response to Acetyl Choline administration compared to control vessels that vasodilate. To further explore the status of the endothelium colleagues performed a detailed histological analysis using electron microscopy. They found that unlike healthy endothelial cells, disease endothelium showed several morphological changes starting from cellular vacuolation, to overt cell death and denudation. Interestingly, statin-treatment improved/retarded the morphological damage of the endothelial cells. Similarly, looking at the endothelial cell junction width they found a gradual increase in junction width in disease animals whereas statin treatment helped to retain junction integrity.

Previously we have shown that an elatin specific MR contrast agent is able to monitor and quantify plaque progression in the brachocephalic artery of atherosclerotic ApoE mice. Uptake of the agent correlated with deposition of elastin as measured by Western Blot. More recently colleagues have developed an MRI method to assess the type of vascular remodeling and was used to image vascular remodelling in the coronary arteries of swine after stent-induced vascular injury. Interestingly, the combination EVG and immunohistological staining for tropoelastin revealed that the net increase in vessel wall elastin is due to the deposition of tropoelastin fibers. When the total elastin content was

measured there was a net increase in elastin fibers in disease compared to control vessels and a slightly higher elastin content in vulnerable compared to stable plaques. However, when only the tropoelastin content was measured there was a significantly higher tropoelastin content in disease compared to control vessels and importantly a higher tropoelastin content in vulnerable compared to stable plaque. If we have a contrast agent that behaved similarly to the antibody we would be able to image vessel wall segments undergoing pathologic elastogenesis since the contribution of the control/mature elastin is almost eliminated. Tropoelastin in all the layers with mature-elastin only in media and adventitia. It would be interesting to look into elastogenesis in the concept of atherosclerosis. For this reason we are working on developing a novel tropoelastin specific agent. Elastin agent have also been used to image cardiac remodeling after myocardial infarction with uptake of the elastin MR agent within the scar and compared to Gd-DTPA. This allowed for a higher CNR between scar and normal myocardium and it also prolonged the acquisition window to 90min compared to 45 min seen with Gd-DTPA.

To extend the extensive discovery programme outlined above to humans, requires in vivo imaging approaches, and optimisation of MR acquisition methodology. An example is the use of 2D Navigator (NAV) to correct respiratory motion during 3D free-breathing whole heart acquisition. This enables simplified scan planning, (no dedicated planning necessary for 2D NAV). 2D NAV directly tracks motion of heart (+no need for 'tracking factor' between diaphragm and heart). It allows respiratory motion tracking in FH and LR direction and improves image quality.

MULTI-SCALE MRI OF THE HEART: MOLECULAR METHODS FOR CELL TRACKING AND TISSUE CHARACTERIZATION

Vandsburger, M. H.

University of Kentucky Physiology and Biomedical Engineering, 741 South Limestone, Lexington, Kentucky 40536, United States

(moriel.vandsburger@gmail.com)

Magnetic resonance imaging (MRI) is an established standard for imaging of cardiac structure and function, and when combined with gadolinium based contrast agents is widely used for imaging of cardiac perfusion and fibrosis in clinical settings and pre-clinical research models. While cardiac MRI is most ubiquitously used to simply obtain high quality anatomical images of the heart, the ability to manipulate the evolution of the magnetic moment through the design of unique pulse sequences opens an array of molecular imaging possibilities using existing MRI hardware. In our lab, we develop cardiac MRI techniques for multi-scale cardiac imaging ranging from multi-color cell tracking to molecular imaging of the tissue microenvironment. For example, we have recently designed a cardiac specific chemical exchange saturation transfer (CEST) pulse sequence, and demonstrated its utility for imaging of the fates of cells labeled with paramagnetic CEST agents in mouse models of cell therapy (Figure 1), and for imaging of myocardial creatine in mouse models of diet induced obesity (1-3). Using similar mechanisms, we have developed an MRI method termed 2-point balanced steady state free precession (bSSFP) that utilizes the exchange of saturated magnetization between extracellular matrix macromolecules and extracellular water to image tissue remodeling utilizing entirely endogenous mechanisms. In an initial clinical study in 47 patients referred for standard of care MRI with gadolinium, 2-point bSSFP demonstrated an excellent association with the identification of infarcted and remodeling myocardium using gadolinium (Figure 2) (4). Recently, we have extended the use of 2-point bSSFP to probe cardiac fibrosis in the setting of end stage renal failure, a patient population at high risk of sudden death but contraindicated to gadolinium. Compared to age matched healthy controls (n = 9), patients with end stage renal failure (n = 13) demonstrate significantly increased fibrotic burden when assessed over the entire heart with 2-point bSSFP. In addition, in 3 patients who have returned for 1 year follow studies, all three demonstrated increased fibrotic burden compared to initial visits, pointing to a possible role of hemodialysis in promoting fibrotic remodeling of the heart. The development of such molecular MRI techniques can enable more robust in vivo studies in pre-clinical models of regenerative medicine, and can be used in clinical settings to identify promising biomarkers, assess the efficacy of emerging therapies, and for longitudinally non-invasive patient monitoring and risk assessment.
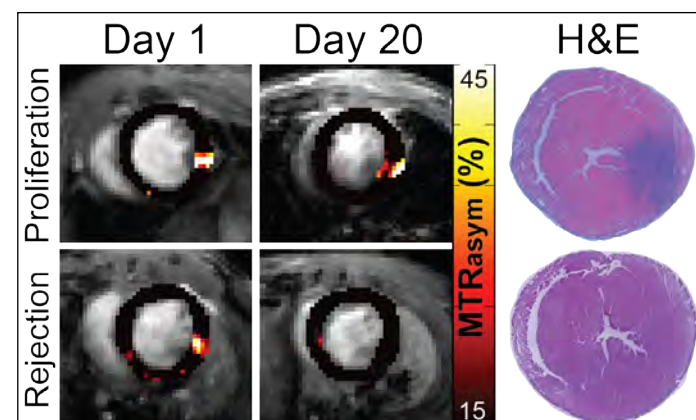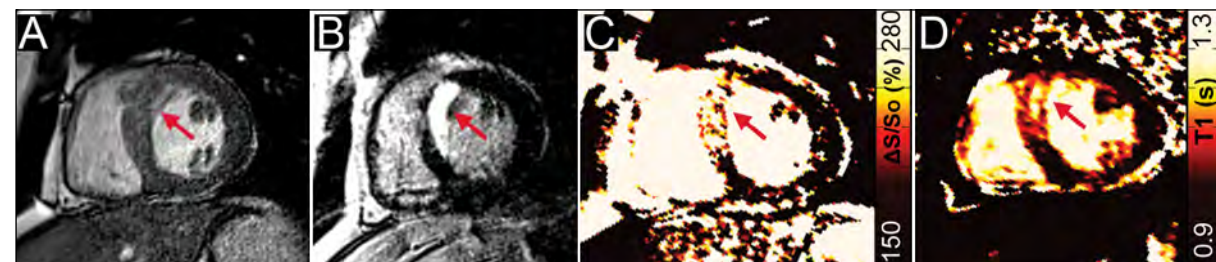
Fig2. Clinical MI imaging: (a) Anatomical image and (b) gadolinium image reveal area of edema confirmed by (c) 2-point bSSFP and (d) native T1-mapping

Figure 1.: CardioCEST tracking of the survival/proliferation (top) or rejection (bottom) of Eu-HPDO3A labeled cells in two mouse models of cardiac cell therapy

TALKS
Thursday, 4 February 2016

APPROACHES TO IMAGE VASCULAR DEVELOPMENT AND DISEASE IN THE MOUSE

Erapaneedi, R.[1,2], Hägerling, R.[1], Pollmann, C.[1], Schäfers, M.[3,2], Kiefer, F.[1,2]

[1]Max Planck Institute Mammalian Cell Signlaing Laboratory, Röntgenstraße 20, 48149 Münster, Germany ; [2]Cluster of Excellence EXC 1003, Cells in Motion, CiM, Waldeyerstraße 15, 48149 Münster, Germany ; [3]European Institute for Molecular Imaging, Waldeyerstraße 15, 48149 Münster, Germany

(fkiefer@gwdg.de)

We are interested in the development, function and pathologies of the vascular systems. Like the neuronal system, the vascular systems function in tissue space, hence a comprehensive 3-dimensional interrogation of their structure and development is paramount to understanding vascular biology.

A few years ago, we started to use a variant of planar illumination microscopy called ultramicroscopy to visualize both the developing blood and lymphatic systems in intact wholemount-stained midgestation mouse fetuses. This analysis revealed that lymphatic endothelial progenitor cells emerge from the largest fetal venous vessel, the cardinal vein, as streams of connected but non-lumenized cells. Our analysis not only resolved a long standing dispute on the mechanism of lymph vessel formation, but also identified novel structures in the developing lymphatic system that had so far eluded the analysis by tissue sections and are only recognized in 3-dimensional renderings.

More recently, we have employed ultramicroscopy to analyse pathologies involving the mature vascular system like atherosclerotic plaques and vessel growth in tumors. During the development of atherosclerosis, macrophages accumulate in the wall of large arterial vessels and initiate a complex set of events, which ultimately leads to the formation of the prototypic atherosclerotic plaque and associated cardiovascular events. While macrophages are a driving force of atherosclerosis, many details of their migratory behaviour during plaque formation remain unknown. Again, we have resided to ultramicroscopy of cleared whole aorta preparations to quantitatively assess the immigration of labelled macrophages into the plaque.

Finally, hypoxia is a major force driving tumor of vascularization, but also associated with the development of treatment resistance. Anti-angiogenic tumor therapies designed to disrupt the tumor vasculature and starve the tumor have largely suffered from poor efficacy, possibly by increasing tumor hypoxia. Despite its central role in tumor biology, but also many other biological processes reporters to image hypoxia in living tissue by optical microscopy at cellular resolution are largely missing. We have developed a novel family of hypoxia reporters that is applicable in intravital imaging and has revealed an unexpected heterogeneity of tumor hypoxic state.

BLI/CT IMAGING OF IFN-B REPORTER MICE REVEALED CONTRIBUTION OF HEPATOCYTES TO IFN-B RESPONSES IN THE LIVER AFTER COXSACKIEVIRUS INFECTION.

Koestner, W.[1,2], Detje, C. N.[2], Lienenklaus, S.[2,3], Langereis, M.[4], Wacker, F.[1], Kalinke, U.[2]

[1]Hannover Medicel School Institute for Radiology, Carl-Neuberg-Str. 1, 30625 Hannover, Germany ; [2]Centre for Experimental and Clinical Infection Research, Twincore Institute for Experimental Infection Research, Feodor-Lynen-Str. 7, 30625 Hannover, Germany ; [3]Hannover Medical School Institute for Laboratory Animal Science, Carl-Neuberg-Str. 1, 30625 Hannover, Germany ; [4]Faculty of Veterinary Medicine, Utrecht University Virology Division, Department of Infectious Diseases and Immunology, Yalelaan 1, Room W507, 3584 CL UTRECHT, Netherlands

(koestner.wolfgang@mh-hannover.de)

Introduction: Coxsackievirus B3 (CVB-3) infection is a frequent cause of human myocarditis. Infection of susceptible mouse strains with CVB-3 results in an acute myocarditis that resembles human myocarditis. Among cytokines that are produced upon CVB-3 infection, IFN-β is a key player. IFN-β binds to the ubiquitously expressed type I IFN receptor (IFNAR) that initiates a defense program to combat viral infection. However, it is still unknown which particular cells are the responsible IFN-β producer during the course of CVB-3 infection that inhibit viral spread. Therefore, we investigated the spatial and temporal distribution of IFN-β induction after CVB-3 infection.

Methods: To visualize IFN-β expression we used luciferase reporter mice (IFN-β $^{\Delta β\text{-luc}}$). In these mice a firefly luciferase was placed under the control of the IFN-β promoter. Two different genetic mouse backgrounds with known differences in susceptibility were studied (Δβ-luc-BALB/c and Δβ-luc-C57BL/6). IFN-β induction after CVB-3 infection was imaged using bioluminescence imaging (BLI).To address whether IFN-β is produced by hepatocytes we investigated hepatocyte-specific reporter mice in which the reporter was activated liver-specifically by intercrossing with alb-cre mice.

Results: In accordance to earlier published results, IFNAR$^{-/-}$-Δβ-luc-mice succumbed within 2 to 3 days after infection. On d 2 p. i., a very strong BLI-signal was observed in the upper abdominal quadrants that colocalized with the liver in cross sectional fused BLI/CT images. The signal strength was enhanced compared with IFNAR$^{+/+}$ Δβ-luc-B6 mice. In Δβ-luc-B6 mice the liver signal reached a maximum on d 2, decreased until d 4, and vanished on d 6 p. i.. Other significant BLI-signals were observed at the cervical region with a maximum at d 3. On d 4 and d 6 p. i., a weak BLI signal was observed in the heart in fused BLI/CT images. In contrast, Δβ-luc-BALB/c mice reached a maximum liver-BLI-signal at d 3 and a maximum cervical-BLI-signal at d 4 p. i., whereas heart-BLI-signals were similar in both strains. Furthermore, signal strength of liver-BLI-signal was enhanced in Δβ-luc-B6 compared with Δβ-luc-B6 mice. After infection of hepatocyte-specific reporter mice, a strong BLI-signal was observed in the liver.

Conclusions: BLI/CT imaging was used to visualize IFN-β induction in liver and heart *in vivo* after CVB-3 infection. Signal strength and spatio-temporal distribution of BLI-signals were identified as biomarkers to discriminate between mouse strains with different susceptibility to CVB-3 infection. Absence of IFNAR resulted in a strong IFN-β response in the liver. The IFN-β response was in part mediated by hepatocytes.

MULTIMODAL NANOPARTICLES FUNCTIONALIZED WITH HUMAN ANTIBODY FRAGMENTS DESIGNED FOR MAGNETIC PARTICLE IMAGING OF ATHEROSCLEROSIS

Lorenzato, C.[1], Larivière, M.[1], Jacobin-Valat, M. - J.[1], Laroche-Traineau, J.[1], Hémadou, A.[1], Adumeau, L.[2], Noubhani, M.[3], Santarelli, X.[3], Ramin, M.[4], Heinen, U.[5], Barthélémy, P.[4], Mornet, S.[2], Clofent-Sanchez, G.[1]

[1]Centre de Résonance Magnétique des Systèmes Biologiques CNRS-UMR5536, 146 rue Léo Saignat, 33076 Bordeaux, France ; [2]ICMCB CNRS-UPR 9048, 87 Avenue du Dr Albert Schweitzer, 33600 Bordeaux, France ; [3]IPB Université de Bordeaux, 146 rue Léo Saignat, 33076 Bordeaux, France ; [4]ARNA laboratory INSERM U869, 146 rue Léo Saignat, Bordeaux, France ; [5]Bruker Biospin, Ettlingen, Germany

(cyril.lorenzato@rmsb.u-bordeaux2.fr)

Introduction: Atherosclerosis, the build-up of lipid-rich atheroma plaques within arterial walls, is a focal trigger of cardiovascular diseases, the pre-eminent killers in the Western world. Atherosclerosis is an inflammatory disease with unstable plaques made of large lipid cores, thin fibrous cap, inflammatory immune cells and platelet infiltrates, making them prone to rupture. Non-invasive molecular imaging modalities based on specific probes will be highly suitable to diagnose instable atheroma plaques. Our purpose was to design a nanoparticle (NP) functionalized with a human antibody (HuAb), TEG4, specific to the platelet αIIbβ3 integrin, and made of both near-infrared fluorescence (NIRF) probes and iron oxide crystals (IOCs) to be tested in fluorescence imaging and used in Magnetic Resonance Imaging / Magnetic Particle Imaging (MPI).

Methods: TEG4 HuAb has been selected by phage display biotechnology.[1] ScFvs (single chain Fragment variable) were processed from the selected phage-HuAbs and produced in *Pichia pastoris*. They were further tested by immunohistochemistry (IHC) on atherosclerotic vessel sections. A site-specific conjugation approach via engineered thiols in scFv fragments was chosen for oriented functionalization of multimodal NPs. Kinetics of binding on αIIbβ3 integrin were determined with Surface Plasmon Resonance (SPR). ApoE$^{-/-}$ mice developing atheroma plaques were injected with NPs grafted with 14 scFv fragments. To satisfy MPI modality, different sizes of IOCs (4 to 11.2 nm) were evaluated *in vitro* by magnetic Particle Spectroscopy (MPS) with an excitation field of 25 mT and a frequency of 25 kHz.

Results: The specificity of TEG4 scFvs has been confirmed in IHC studies on murine, rabbit and human lesional tissue rich in platelets. SPR analyses of scFv-NPs grafted with increasing numbers of scFvs showed a gradual increase in the avidity (Fig. 1). The same was true regarding the intensity of atheroma plaque recognition in IHC. *In vivo* homing of multimodal NPs grafted with 14 scFv fragments was visualized by fluorescence tomography. MPS measurements (Fig. 2) showed a clear improvement of the potential MPI signal with the increase of IOCs.

Conclusions: When multiple copies of scFv fragments were grafted to NPs, the avidity was increased. This enabled the NPs to reach its target protein *in vivo*, given the encouraging results of NIRF imaging in ApoE$^{-/-}$ mice. The multifunctional feature of these NPs allows the development of a set of complementary imaging techniques at multiple scales from cell to animal. As a perspective, we plan on doing MPI *in vivo* experiments with NP functionalized with TEG4 and including 17 nm sized IOCs allowing for higher MPI resolutions.[2]

References: 1. Jacobin MJ, Laroche-Traineau J, Little M, Keller A, Peter K, Welschof M, et al. Human IgG monoclonal anti-alpha(IIb)beta(3)-binding fragments derived from immunized donors using phage display. *J Immunol* 2002;168:2035-2045. 2. Starmans LW, Burdinski D, Haex NP, Moonen RP, Strijkers GJ, Nicolay K, et al. Iron oxide nanoparticle-micelles (ION-micelles) for sensitive
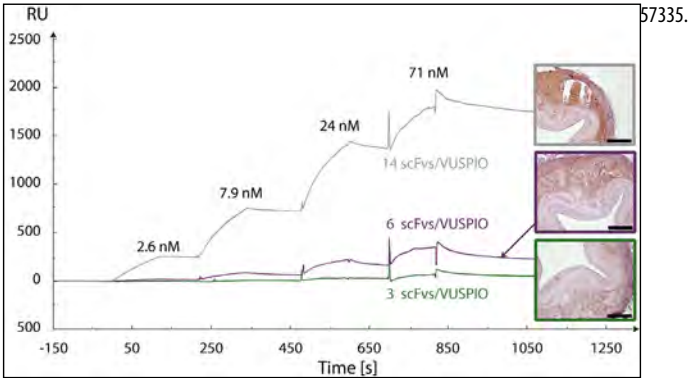

Figure 1: The reactivity against αIIbβ3 integrin was found to be gradually improved when increasing the number of scFvs grafted per VUSPIO, as shown here by SPR (concentrations from 2.6 to 71 nM) and IHC analyses.
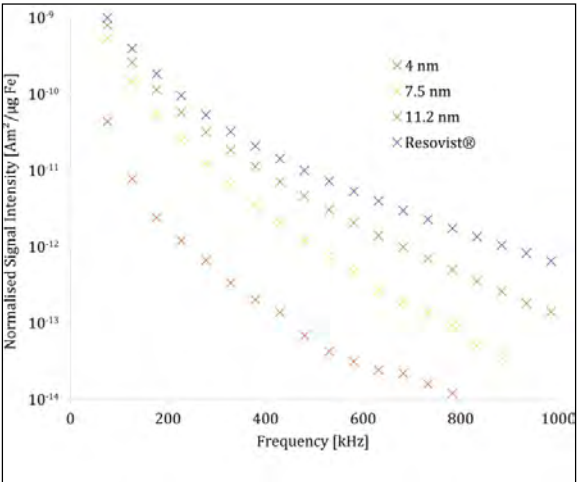

Figure 2: MPS harmonic spectra of multimodal NPs of 100 nm (hydrodynamic diameter) for different sizes of iron oxide crystal (4 nm, 7.5 nm and 11.2 nm). All spectra were normalized by the iron concentration

OPTICAL AND OPTOACOUSTIC METHODS FOR NEXT-GENERATION CARDIOVASCULAR IMAGING

Ntziachristos, V.[1,2]

[1]Technische Universität München Lehrstuhl für Biologische Bildgebung, Ismaninger Str. 22, 81675 München, Germany ; [2]Helmholtz Zentrum München Institut für Biologische und Medizinische Bildgebung, Ingolstädter Landstr. 1, 85764 Neuherberg, Germany

(v.ntziachristos@helmholtz-muenchen.de)

Optical imaging is unequivocally the most versatile and widely used visualization modality in the life sciences. Yet it is significantly limited by photon scattering. For the past few years there has been an emergence of powerful new optical imaging methods that can offer high resolution imaging beyond the penetration limits of microscopic methods. Of particular importance is the development of multi-spectral opto-acoustic tomography (MSOT) that brings unprecedented optical imaging performance in visualizing anatomical, physiological and molecular imaging biomarkers. Some of the attractive features of the method are the ability to offer 10-100 microns resolution through several millimetres to centimetres of tissue and real-time imaging. In parallel we have achieved the clinical translation of targeted fluorescent probes, which opens new ways in the diagnosis and treatment of cardiovascular disease and inflammation. This talk describes current progress with methods and applications for in-vivo optical and opto-acoustic imaging and outlines how new opto-acoustic and fluorescence imaging concepts are necessary for accurate and quantitative molecular investigations in tissues.

HIGH FRAME-RATE PHOTOACOUSTIC IMAGING OF OXYGEN SATURATION IN THE MOUSE MYOCARDIUM USING ECG-GATED KILOHERTZ VISUALIZATION

Forbrich, A.[1], Warren, C.[1], Trochet, P.[2], Jose, J.[2], Heinmiller, A.[1]

[1]FUJIFILM VisualSonics, Inc., 3080 Yonge St, Suite 6100, Toronto Ontario M4N 3N1, Canada ; [2]FUJIFILM VisualSonics, Inc., Joop Geesinkweg 140, 1114 AB Amsterdam, Netherlands

(aheinmiller@visualsonics.com)

Introduction: As cardiovascular disease is the number one cause of death worldwide [1], basic research into the biology of the disease is imperative. High-frequency ultrasound imaging is a valuable tool for assessing small animal models of cardiovascular disease, however there remain some limitations to functional assessment of the myocardium, since most measurements are based on mechanical properties of the muscle. Photoacoustic (PA) imaging is a hybrid optical and ultrasound imaging modality that uses pulsed laser light to visualize blood and measure oxygen saturation (sO_2) levels. The slow pulse repetition rate of commonly used lasers for PA, relative to the fast heart rates in mice remains a challenge for accurate PA imaging. The aim of this study is to apply retrospective processing known as ECG-Gated Kilohertz Visualization (EKV)[2]to PA cardiac imaging, overcoming timing challenges and allowing for the visualization of s O_2 throughout the full cardiac cycle, with high temporal resolution.

Methods: A preclinical high-frequency ultrasound and PA imaging system (Vevo LAZR, FUJIFILM VisualSonics, Inc., Toronto, Canada) was used to collect radio frequency (RF) data of the anterior myocardium of CD-1 mice. PA images of the long axis of the heart at 750 and 850 nm were visualized using a 21 MHz linear array transducer (LZ-250, FUJIFILM VisualSonics, Inc., Toronto, Canada). To assess s O_2 measurements, the mouse was imaged while breathing first medical air (20% O_2) then100% O_2. The data was analyzed offline in Matlab using two different algorithms: frame averaging and the EKV technique.sO_2 was calculated according to the procedure described in [3].

Results: The EKV processing technique resulted in higher quality images than frame averaging. The major movement of the heart from frame to frame combined with the large amount of frames being averaged caused extensive blurring. The s O₂ images retrospectively processed using EKV were more localized, with higher spatial and temporal resolution. Using the latter method, 100 frames per mouse cardiac cycle were obtained.

Conclusions: Applying EKV processing to PA cardiac images can be used to measure s O₂ in the heart, which could be useful for investigating cardiovascular events in small animals such as measuring the size of a myocardial infarction. With larger buffer sizes it is expected that even higher frame rates are possible. Further information could potentially be provided by 3D EKV processing of PA cardiac images, which will be the subject of future studies.

References: [1] Preventing chronic disease: a vital investment. Geneva, World Health Organization, 2005. [2] Cherin, E., Williams, R., Needles, A., Liu, G., Brown, A.S., Zhou, Y.Q., Foster, F.S. (2006) Ultrahigh frame rate retrospective ultrasound microimaging and blood flow visualization in mice in vivo. *Ultrasound Med Biol., 32(5)*, 683-91. [3] Wang, X., Xie, X., Ku, G., Wang, L. (2006). Noninvasive imaging of hemoglobin concentration and oxygenation in the rat brain using high-resolution photoacoustic tomography. *Journal of Biomedical Optics, 11(2)*, 024015.
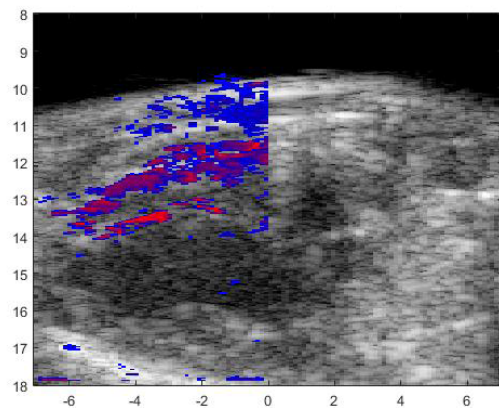
Persisted mouse heart: A single frame of a persisted mouse heart showing oxygen saturation as a parametric map with red being high sO2 and blue being low sO2
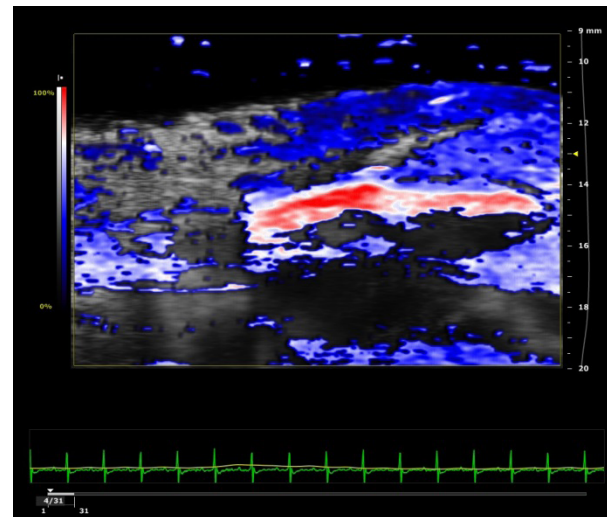
EKV processed mouse heart: A single frame of an EKV processed mouse heart showing oxygen saturation as a parametric map with red being high sO2 and blue being low sO2

THE CHALLENGE OF IMAGING THE MOVING HEART WITH POSITRON EMISSION TOMOGRAPHY: MOTION COMPENSATION STRATEGIES FOR QUANTITATIVE DATA ANALYSES.

Schäfers, K.

University of Münster European Institute of Molecular Imaging, Waldeyer Str. 15, 48149 Münster, Germany

(schafkl@uni-muenster.de)

Imaging the heart with positron emission tomography is a challenging task due to several reasons. (1) The structures of interest, e.g. the left and right myocardial walls, are small compared to the limited spatial resolution of a PET scanner leading to partial volume effects. (2) The heart beat causes blurring of imaging structures. (3) The heart is tilted due to the respiratory action of the diaphragm. Since the spatial resolution of PET has been substantially improved over the past decades, motion has been exposed to be a major source of image degradation and may thus hamper a proper data quantification. Several motion compensation strategies have been followed to overcome the motion blurring problem in PET. Tracer kinetic modelling approaches usually try to model the motion-induced spillover-effects and incorporate a motion compensating term into the modelling equation. In hybrid PET/CT imaging, the motion information is commonly derived from the PET data itself by dividing and reconstructing the acquired list-mode raw data into respiratory or cardiac gates on which the motion is estimated. Using these motion vector fields, a motion-compensated image reconstruction (MCIR) can be performed by transforming all data to a reference motion-frozen state (e.g. end-expiration, end-diastole). Ideally, both cardiac and respiratory motion has to be taking into account in a dual-gating MCIR approach. Fig. 1 is demonstrating such a motion compensation strategy for F-18 FDG data of the myocardium leading to a clear improvement in assessing wall thickness and myocardial uptake while restoring the full data statistics (data from Gigengack et al. TMI 2012)

With the invention of hybrid PET/MR scanners, new motion compensation strategies could be followed using the MR as a source for gathering motion information. The hybrid PET and MR approach allows to collect motion information in parallel to the PET raw data acquisition. The excellent soft-tissue contrast of MRI enables to extract highly accurate motion vector fields leading to improved motion-compensated PET images. This is especially true for the complex motion of the myocardium which can hardly be described by parameters derived from PET raw data itself. Therefore, hybrid PET/MR offers new ways of improved cardiac molecular imaging which may have an impact on future diagnostic strategies.

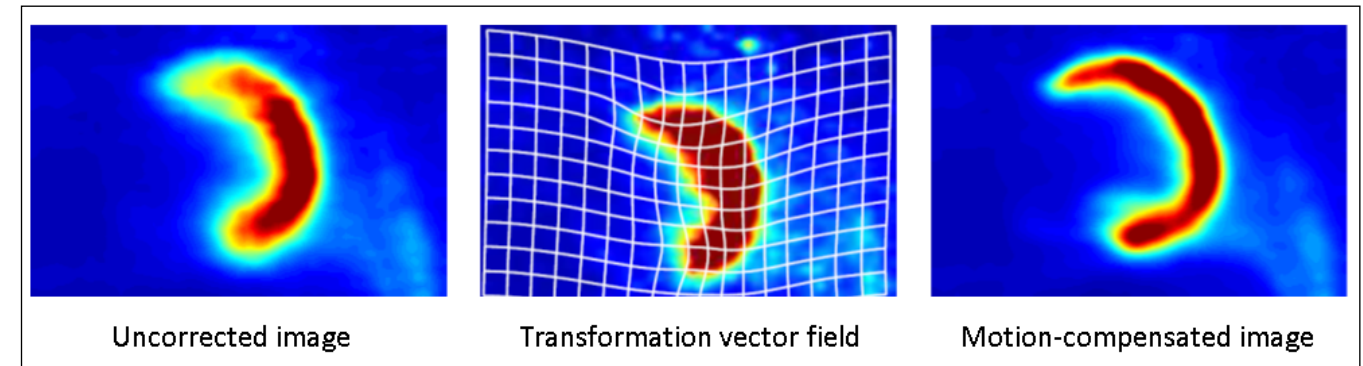Uncorrected image   Transformation vector field   Motion-compensated image

Fig. 1: Dual-gated motion-compensated PET image reconstruction showing clear improvement in visualized cardiac tracer uptake after motion correction.

IN VIVO QUANTITATIVE ASSESSMENT OF MYOCARDIAL STRUCTURE, FUNCTION, PERFUSION AND VIABILITY USING CARDIAC MICRO-COMPUTED TOMOGRAPHY.

Van Deel, E.[1,2], Ridwan, Y.[2], Belenkov, S.[3], Essers, J.[2,4,5]

[1]Erasmus MC Cardiology, Dr. Molewaterplein 50, 3015GE Rotterdam, Netherlands; [2]Erasmus MC Genetics, Dr Molewaterplein 50, 3015GE Rotterdam, Netherlands; [3]Perkin Elmer, Waltham, MA United States; [4]Erasmus MC Vascular Surgery, Dr. Molewaterplein 50, 3015 Rotterdam, Netherlands; [5]Erasmus MC Radiation Oncology, Dr. Molewaterplein 50, 3015GE Rotterdam, Netherlands

(sasha.belenkov@perkinelmer.com)

Introduction: In this study, we used a high-speed MicroCT system with intrinsic cardio-respiratory gating, in conjunction with blood-pool iodinated contrast agent, for determining myocardial global and regional function along with myocardial perfusion and viability in healthy mice and in a cardiac ischemia mouse model induced by permanent occlusion of the left anterior descending coronary artery (LAD).

Methods: Four C57Bl/6 mice, three with LAD occlusion and one sham-operated completed the imaging protocol which consisted of a single contrast agent intravenous bolus administration and two 4.5-min cardio-respiratory MicroCT acquisitions. Threshold-based 3D segmentations of the left ventricular cavity were performed on both end-diastolic and end-systolic volumes to determine left ventricular end-diastolic volume (LVEDV) and left ventricular end-systolic volume (LVESV) which were then used to calculate left ventricular ejection fraction (LVEF) and cardiac output (CO). Epicardial contour segmentations were performed to allow subdivision of the myocardium into 16 segments with subsequent calculation of regional left ventricular wall motion abnormality (LVWM), left ventricular wall thickening (%LVWTh), ejection fraction (%EF), contrast perfusion and uptake. In addition, left ventricular myocardial mass (LVMM) and myocardial infarct size (%LVMIS) were determined.

Results: Three hours after the ligation, the mean LVEDV was not different between the myocardial infarction group and the sham-operated animal (2.8 ± 0.23 vs. 2.3). However, the body weight normalized mean LVESV was higher in the myocardial infarction group (2.1 ± 0.31 vs. 0.92). Correspondingly, the mean LVEF and cardiac output (CO) in mice with LAD coronary artery occlusion were lower when compared to the sham-operated mouse (23.1% ± 7.1% vs. 60.5%, and 0.26mL ± 0.08mL vs. 0.55mL respectively). Quantitative assessment of LV myocardial mass and infarction size indicated that 22.4 %, 13.3%, and 15.8% of the left ventricular myocardial mass was affected in mouse 1, 2, and 3 respectively. The LV wall motion, thickening, regional ejection fraction, contrast perfusion and uptake scores showed that LAD coronary artery ligation resulted in marked decrease of LV regional functional indices, whereas no effect was observed in the sham-operated mouse.

Conclusions: This work has demonstrated the first successful use of a high-speed MicroCT system for comprehensive determination of myocardial global and regional functional parameters along with assessment of myocardial perfusion and viability in healthy and in a mouse model of myocardial infarction. The technique can be performed to evaluate novel preventive and therapeutic strategies.
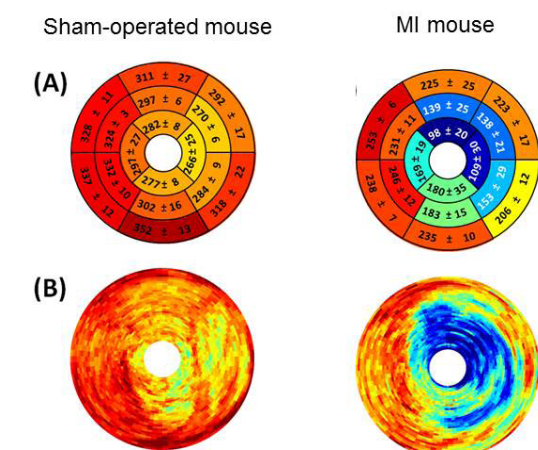
Sham-operated mouse   MI mouse

(A)

(B)

Fig. 1: Myocardial perfusion plot: Representative end-diastolic circumferential polar plot displays (Bulls Eye polar plots) of myocardial perfusion in a mouse without myocardial infarction (sham-operated mouse) and a mouse with myocardial infarction (MI mouse).

Representative end-diastolic circumferential polar plot displays (Bulls Eye polar plots) of myocardial perfusion in a mouse without myocardial infarction (sham-operated mouse) and a mouse with myocardial infarction (MI mouse). (A) The left ventricle is subdivided into basal, mid-cavity, and apical short-axial portions according to the 17-segment AHA model. Dissimilar perfusion is clearly visible in mid-anterior, mid-inferolateral, mid-anterolateral, apical anterior, and apical lateral segments in the MI mouse compared to the sham-operated mouse. Values shown represent the segmental means in Hounsfield units ± standard deviations. (B) Myocardial perfusion maps are shown without subdivision into 17 segments. The center of the plot corresponding to the cardiac apex (segment 17) is not shown.

ASSESSMENT AND PRECISE QUANTIFICATION OF POST-INFARCTION SCAR REMODELING USING THE CONTRAST AGENT GADOFLUORINE P AND T1 MAPPING TECHNIQUES

Lohöfer, F.[1], Hoffmann, L.[1], Glinzer, A.[1], Kosanke, K.[1], Schilling, F.[2], Rummeny, E.[1], Wildgruber, M.[1]

[1]TU Muenchen Radiology, Ismaninger Straße 22, 81675 Muenchen, Germany ; [2]TU Muenchen Nuclear Meedicine, Ismaninger Straße 22, 81675 Muenchen, Germany

(fabian.lohoefer@tum.de)

Introduction: The aim of this study is to evaluate molecular magnetic resonance imaging (MRI) at high field strength using a collagen-targeted contrast agent to analyze and quantify mechanisms of myocardial remodeling and scar formation in a murine myocardial infarction model.

Methods: In-vivo accumulation of Gadofluorine P, targeting collagen, tenascin and proteglycans within the infarct scar, was investigated in a mouse model of myocardial infarction. C57BL/6J mice were scanned by in-vivo MRI at 7 Tesla 1 and 6 weeks after coronary artery ligation. Gadofluorine P was injected at a dose of 0.1mmol/kg body weight and compared to conventional Gd-DTPA. Contrast enhancement of infarcted myocardium was assessed using Late Gadolinium Enhancement (LGE) and T1 mapping. T1/R1 values were calculated from T1 maps based on a Look-Locker sequence. T1 images were calculated from source images based on a 3-parameter Levenberg-Marquardt curve fitting procedure with a correction for read-out-induced attenuation of the relaxation curve. Cardiac function parameters were assessed by volumetric analysis based on short axis views in CINE sequences. Mice from each time point were sacrificed after completion of imaging. The heart was removed and further processed for immunohistochemistry and matrix-assisted laser desorption ionization imaging (MALDI) to quantify Gadofluorine P accumulation ex-vivo.

Results: R1 values in myocardial infarction peaked 10min after Gadofluorine P injection. A slow linear decrease was seen over a time period of 2h. CNR between infarcted and healthy myocardium in LGE reached baseline values after 90 min, whereas R1 values of infarcted tissue were still significantly increased. Especially mice with high initial R1 values following Gadofluorine P injection developed progressive heart failure with extensively reduced ejection fraction after 6 weeks.

Conclusions: MR imaging using the collagen-targeted contrast agent Gadofluorine P allows capturing of extracellular matrix components in remodeling and scar formation after myocardial infarction. T1 mapping at high field strength enables a more precise quantification of signal enhancement and imaging over a prolonged time period compared to conventional LGE.

MULTIMODALITY IMAGING REVEALS INCREASED MATRIX METALLOPROTEASE ACTIVITY AND APOPTOSIS PRECEDING CARDIAC FAILURE IN PROGEROID ERCC1 MICE

Van Thiel, B.[1,2,3], De Boer, M.[4], Ridwan, Y.[1], De kleijnen, M.[4], Danser, J.[3], Duncker, D.[4], Van der Pluijm, I.[1,2], Essers, J.[5,1,2]

[1]Erasmus MC Genetics, Dr Molewaterplein 50, 3015GE Rotterdam, Netherlands; [2]Erasmus MC Vascular Surgery, Dr. Molewaterplein 50, 3015 Rotterdam, Netherlands; [3]Erasmus MC Pharmacology, Dr. Molewaterplein 50, 3015GE Rotterdam, Netherlands; [4]Erasmus MC Cardiology, Dr. Molewaterplein 50, 3015GE Rotterdam, Netherlands; [5]Erasmus MC Radiation Oncology, Dr. Molewaterplein 50, 3015GE Rotterdam, Netherlands

(j.essers@erasmusmc.nl)

Introduction: In this study, we tested the use of functional micro-Computed Tomography (MicroCT) imaging combined with near infrared fluorescent (NIRF) probes to directly report the *in vivo* activity of key biomarkers of age-related cardiac failure using progeroid Ercc1 mouse models. Mutations in the ERCC1 gene causes diminished DNA damage repair and an accelerated aging phenotype in mice, including cardiovascular aging. We tested the effect and kinetics of diminished DNA damage repair on protease activity and apoptosis and possible subsequent cardiac failure *in vivo*.

Methods: Full body Ercc1[D/-], cardiomyocyte-specific Ercc1[c/-] and their wild-type controls were imaged with contrast enhanced MicroCT for anatomical reference and to assess cardiac morphology and function. The NIRF probes MMPSense680™ and Annexin-Vivo750™ were used to image matrix metalloprotease activity and apoptosis, respectively. Functional microCT analysis was compared to ultrasound imaging and results were validated by histology.

Results: Full body Ercc1[D/-] mice display increased *in vivo* apoptosis in their myocardium at 18 weeks of age compared to WT (Ercc1[D/-] 39+/-2 pmol vs WT 5+/-2 pmol; $p<.01$; n=5 vs n=4), which was also shown at 12 weeks of age and confirmed by histology. *Ex vivo* matrix metalloprotease activity in these mice was increased at 12 weeks of age (Ercc1[D/-] 14 +/-6 pmol/g vs WT 0.1+/-0 pmol/g; n=7 vs n=6), though decreased at 18 weeks (Ercc1[D/-] 3+/-2 pmol/g; n=5) compared to 12 week old Ercc1[D/-]. However, no significant decline in cardiac function was observed in these Ercc1[D/-] mice. Cardiomyocyte-specific deletion of Ercc1 also led to increased myocardial apoptosis (Ercc1[c/-] 24+/-3 pmol vs WT 6+/-1 pmol; $p<.05$; n=4 vs n=3) but conversely also loss of cardiac function shown by increased diastolic LV volume (Ercc1[c/-] 76+/-6 mm³ vs WT 56+/-4 mm³; $p<.05$; n=4 both groups) and decreased ejection fraction (Ercc1[c/-] 30%+/-2 vs WT 53%+/-2; $p<.05$; n=4 both groups).

Conclusions: In conclusion, combined CT and optical imaging allows simultaneous analysis of molecular and functional changes in mouse models for accelerated aging and shows that temporal increase in matrix metalloprotease activity is followed by apoptosis and cardiac functional decline in progeroid Ercc1 mice.

IMAGING THE ROLE OF AKT1 IN ANGIOGENESIS AND CARDIOVASCULAR DISEASE

Neeman, M.

Weizmann Institute Biological Regulation, Herzel, 76100 Rehovot, Israel

(michal.neeman@weizmann.ac.il)

Akt1 is a serine-threonine protein kinase, which serves as a key signaling hub in the phosphatidylinositol 3-kinase (PI3K) pathway, mediating the response to many growth factors. This pathway is important in regulating metabolism, proliferation, cell survival, growth and angiogenesis. Over the last years we studied the role of Akt1 on development using mice deficient in Akt1 and mice selectively over expressing Akt1, with a particular focus on the application of dynamic contrast enhanced MRI for mapping vascular remodeling. These studies demonstrated the importance of Akt1 on vessel permeability and capillary expansion. Akt1 deficiency was associated with reduced survival due to placental hypovascularity. Intra uterine growth retardation was attributed to reduced vascularity of the long bones. The heart showed reduced vascularity, but surprisingly Akt1 deficient mice showed enhanced recovery after experimental myocardial infarction, apparently due to preconditioning incudes by Akt1 deficiency. Ovarian grafts derived from Akt1 deficient mice show enhanced follicular degeneration and loss of the oocyte reserve. In contrast, inducible over expression of Akt1 resulted in enhanced vascular permeability and angiogenesis, suggesting that Akt1 was necessary and sufficient for regulating vascular remodeling. In ovarian grafts, transient genetic or pharmacologic induction of endothelial expression of Akt1 was sufficient for enhancing graft survival.

In summary, contrast enhanced MRI was instrumental in delineating the central role of Akt1 in vascular remodeling

Publications: 1.   Thuy L. Phung, Keren Ziv, Donnette Dabydeen, Godfred Eyiah-Mensah, Marcela Riveros, Carole Perruzzi, Jingfang Sun, Rita A. Monahan-Earley, Ichiro Shiojima, Janice A. Nagy, Michelle I. Lin, Kenneth Walsh, Ann M. Dvorak, David M. Briscoe, Michal Neeman, William C. Sessa, Harold F. Dvorak, and Laura E. Benjamin. Pathological angiogenesis is induced by sustained Akt signaling and inhibited by rapamycin. Cancer Cell 10, 159–170, 2006 2.   Katrien Vandoorne, Jeremy Magland, Vicki Plaks, Amnon Sharir, Elazar Zelzer, Felix Wehrli, Brian A. Hemmings, Alon Harmelin and Michal Neeman. Bone vascularization and trabecular bone formation are mediated by PKBalpha/Akt1 in a gene dosage dependent manner: In vivo and ex vivo MRI. Magn Reson Med, 2010 Jul;64(1):54-64. 3.   Plaks V, Berkovitz E, Vandoorne K, Berkutzki T, Damari GM, Haffner R, Dekel N, Hemmings BA, Neeman M, Harmelin A. Survival and Size Are Differentially Regulated by Placental and Fetal PKBalpha/AKT1 in Mice. Biol Reprod. 2011 Mar;84(3):537-45. Epub 2010 Oct 27. 4.   Katrien Vandoorne, Moriel H. Vandsburger, Tal Raz, Moran Shalev, Karen Weisinger, Inbal Biton, Vlad Brumfeld, Calanit Raanan, Nava Nevo, Raya Eilam, Brian A. Hemmings, Eldad Tzahor, Alon Harmelin, Lior Gepstein, Michal Neeman. Chronic Akt1 deficiency attenuates adverse remodeling and enhances angiogenesis after myocardial infarction. Circulation: Cardiovascular Imaging, 2013 Nov;6(6):992-1000. 5.   Vandoorne, Katrien, Vandsburger, Moriel, Brumfeld, Vlad, Hemmings, Brian, Harmelin, Alon, Neeman, Michal. Multimodal imaging reveals a role for Akt1 in fetal cardiac development. Physiol Rep. 2013 Nov;1(6):e00143. doi: 10.1002/phy2.143. Epub 2013 Nov 7. 6.   Yoni Cohen, Hagit Dafni, Reut Avni, Tal Raz, Inbal Biton, Brian Hemmings, and Michal Neeman. In search of signaling pathways critical for ovarian graft reception: Akt1 is essential for long- term survival of ovarian grafts. Fertility and Sterility 2014 Feb;101(2):536-44. 7.   Cohen Y, Dafni H, Avni R, Fellus L, Bochner F, Rotkopf R, Raz T, Benjamin LE, Walsh K, Neeman M. Genetic and Pharmacological Modulation of Akt1 for Improving Ovarian Graft Revascularization in a Mouse Model. Biol Reprod. 2015 Oct 21. pii: biolreprod.115.131987. [Epub ahead of print] PMID: 26490838

TALKS

CARDIAC TISSUE CHARACTERIZATION BASED ON ULTRASOUND IMAGING OF THE PHYSICS

De Jong, N.[1], Vos, H. J.[1], Strachinaru, M.[1], Van Dalen, B. M.[1], Verweij, M.[2]

[1]Erasmus MC Biomedical Engineering, Rotterdam, Netherlands; [2]Delft University of Technology Laboratory of Acoustical Wavefield Imaging, dept. Imaging Physics, Delft, Netherlands

(n.dejong@erasmusmc.nl)

Heart failure is a disease in which the heart cannot supply sufficient blood to the body, especially during activity. One flavour of the disease, diastolic heart failure, occurs with increasing age, reaching > 5% of occurrence for those of aged >70 yrs, and therefore is an increasing problem. The main cause of the disease is a stiffening heart muscle. Yet, even modern cardiology lacks a sensitive method to measure the muscle stiffness in a patient-friendly manner. Therefore we are developing new methods to measure the stiffness non-invasively with medical ultrasound. We reason that the stiffness determines the propagation velocity of shear waves (1 – 10 m/s in soft biological tissue). By imaging the shear waves, we estimate the stiffness. Shear waves occur naturally on the heart, and can also be induced. Both methods will be presented with application to skeletal and cardiac muscle.

The physics behind the waves in a complex geometry such as the heart will be addressed through numerical modelling, in-vitro testing, animal studies, and volunteer study results. First, the numerical modelling exists of both an analytical model of Lamb waves in a visco-elastic plate in a liquid surrounding, and numerical finite difference calculations thereof. Second, we will show the ultrasound-tracked shear waves in a phantom, which are induced by a strong ultrasound push pulse. Third, we will show the experimental data from a large animal (pig) study, in which we tested several automated detection schemes to extract the propagation velocity of shear waves in the heart after the closure of the valves. These coincide with the audible heart tones. We will also show the recordings made from open-chest ultrasound experiments, in which blood flow inside the left ventricle is clearly identified, including other dynamic motion of valves, the cardiac tissue, etc. Finally, we will show experimental results of skeletal muscle in contracted and relaxed state, and the results of healthy volunteer recordings. The phenomena will be illustrated with ultrasound movies.
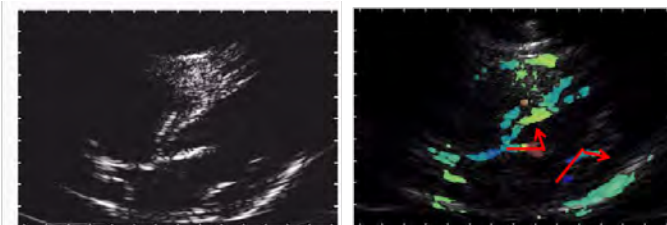
B-mode image & tissue: B-mode image & tissue velocity image obtained with lag-one phase correlation technique
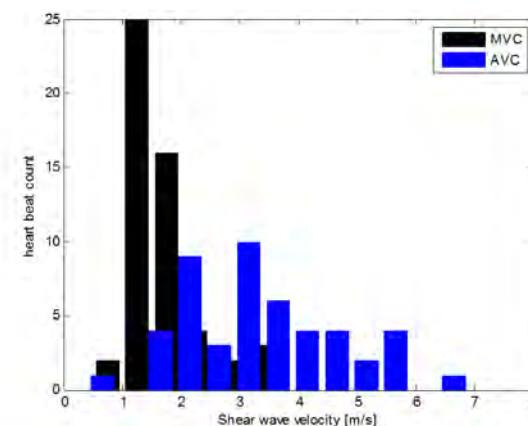
Shear wave: Shear wave velocities measured in 22 pigs after mitral valve closure (MVC) and aortic valve closure (AVC)

MOLECULAR ULTRASOUND IMAGING OF AᵥB₃-INTEGRIN EXPRESSION IN CAROTID ARTERIES OF PIGS AFTER VESSEL INJURY

Rix, A.[1], Fokong, S.[1], Heringer, S.[2], Pjontek, R.[2], Nonn, A.[2], Theek, B.[1], Wiesmann, M.[2], Kiessling, F.[1]

[1]RWTH Aachen experimental molecular imaging, Pauwelsstrasse, 52074 Aachen, Germany ; [2]RWTH Aachen Diagnostic and Interventional Neuroradiology, Pauwelsstrasse, 52074 Aachen, Germany

(arix@ukaachen.de)

Introduction: Endovascular interventions like balloon angioplasty can cause vascular injury leading to platelet activation, thrombus formation and inflammatory response. This induces smooth muscle cell (SMC) activation and subsequent re-endothelialization with expression of $\alpha_v\beta_3$-Integrin by SMC's and endothelial cells[1,2]. Thus, vascular healing after vessel injury in pigs was evaluated by molecular ultrasound imaging with polybutyl-cyanoacrylate microbubbles (MB) targeted to $\alpha_v\beta_3$-Integrin.

Methods: Approval for animal experiments was obtained. The binding specificity of $\alpha_v\beta_3$-Integrin targeted MB to HUVEC was tested using fluorescence microscopy. In vivo imaging was performed using a clinical ultrasound system and a 8MHz probe. 6 minipigs were examined after vessel injury in the left carotid artery. The right carotid served as control. Uncoated MB, unspecific cDRG-coated MB, and $\alpha_v\beta_3$-Integrin specific cRGD-coated MB were injected. Bound MB were assessed 8 min after injection using ultrasound replenishment analysis. Measurements were performed 2 hours, 1 and 5 weeks and 3 and 6 months after injury. In vivo data were validated by immunohistochemistry.

Results: Significantly stronger binding of cRGD-MB than MB and cDRG-MB to HUVEC was found (p<0.0001). As vessel injury lead to upregulation of $\alpha_v\beta_3$-Integrin, cRGD-MB (SI bound MB: 5.12 ± 1.46 a.u.) bound significantly stronger (p<0.01) in the injured carotid arteries compared to unspecific cDRG-MB and uncoated MB (SI bound MB: cDRG-MB: 0.47 ± 0.86 a.u.; MB: 0.65 ± 1.14 a.u.) , as well as compared to bound cRGD-MB at the counterside carotid artery (SI bound MB 0.78 ± 0.59 a.u.) 1 week after vessel injury. After 3 months $\alpha_v\beta_3$-Integrin expression decreased to baseline and binding of cRGD-MB was comparable in both vessels.

Conclusions: Ultrasound imaging with RGD-PBCA-MB is promising for monitoring vascular healing after vessel injury. This may open new perspectives to assess vascular damage after radiological interventions and to monitor anti-inflammatory vascular therapies.

NONINVASIVE MOLECULAR ULTRASOUND MONITORING OF ENDOTHELIAL RECOVERY FOLLOWING INTRAVASCULAR SURGICAL PROCEDURES FOR REVASCULARISATION

Curaj, A.[1,2], Wu, Z.[1,2], Fokong, S.[1], Liehn, E.[2], Weber, C.[3], Burlacu, A.[4], Lammers, T.[1], Van Zandvoort, M.[5], Kiessling, F.[1]

[1]RWTH Institute for Experimental Molecular Imaging, Aachen, Germany ; [2]RWTH Institute for Molecular Cardiovascular Research, Aachen, Germany ; [3]Ludwig-Maximilians-University Munich Institute of Cardiovascular Prevention, Germany ; [4]Institute of Cellular Biology and Pathology "Nicolae Simionescu" of the Romanian Academy Institute of Cellular Biology and Pathology "Nicolae Simionescu", Bucharest, Romania ; [5]Maastricht University Dep. of Genetics and Molecular Cell Biology, School for Cardiovascular Diseases CARIM, Maastricht, Netherlands

(acuraj@ukaachen.de)

Introduction: During catheter-based interventions, vascular endothelium is injured making antithrombotic therapy inevitable until complete endothelial recovery. Therefore, many patients undergo prolonged anticoagulation therapy, denying them any invasive medical procedures, such as surgical operations and dental interventions. We aim to introduce molecular ultrasound (US) imaging of the vascular cell adhesion molecule (VCAM)-1 using targeted microbubbles (MB$_{VCAM-1}$) as an easy accessible, cheap and real-time imaging modality, to accurately monitor the reendothelialization of vessels.

Methods: ApoE−/− mice fed with an atherogenic diet for 1 and 12 weeks were subjected to left common carotid artery endothelial denudation. Molecular US and Two-photon laser scanning microscopy (TPLSM) imaging were performed at different time points after denudation (1, 3, 7, and 14 days) to investigate VCAM-1 availability for targeting during endothelial recovery.

Results: After arterial denudation, an increased MB$_{VCAM-1}$ binding after 1 day (d), a peak after 3d, and a decrease after 7d was found (Fig1). In the short term diet group (1 week before the intervention), quantification of MB$_{VCAM-1}$ binding showed a ~8-fold increase in US grayscale intensity after 1d, a ~15-fold increase after 3d, and only a ~2-fold increase after 7d compared to noninjured carotids. Fourteen days post intervention, MB$_{VCAM-1}$ binding returned to the level of healthy controls. Ex vivo TPLSM of denudated arteries confirmed VCAM-1 luminal exposure from remaining endothelial cells (ECs) and exposed vascular smooth muscle cells at 1 and 3d after arterial denudation (Fig2A). After complete reendothelialization, VCAM-1 expression persisted in the subendothelial layer but was not accessible for the MB$_{VCAM-1}$ anymore (Fig2B and C). In the long term diet group (12 weeks of diet), MB$_{VCAM-1}$ binding also peaked after 3d showing an ~18-fold increase in US grayscale intensity but remained high until 7d (~8-fold increase), indicating a delay in endothelial recovery (Fig1).

Conclusions: Molecular US imaging with MB$_{VCAM-1}$ is promising to faithfully depict vessel damage and monitor endothelial regeneration after arterial interventions. Therefore, we hypothesize that molecular US imaging may become a powerful diagnostic tool to personalize therapy after vascular interventions, capable of improving the therapeutic outcome and discriminate the possibility of invasive procedures in patients with acute associated pathologies.
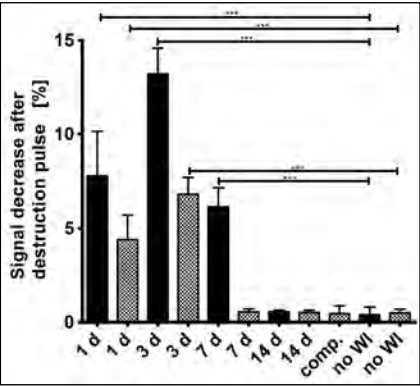
In vivo molecular US: The quantification and statistical analysis of MB binding indicates specific binding of MBVCAM-1 to denudated carotid arteries (1 week high cholesterol diet—chess pattern bars, 12 weeks high cholesterol diet—solid bars).
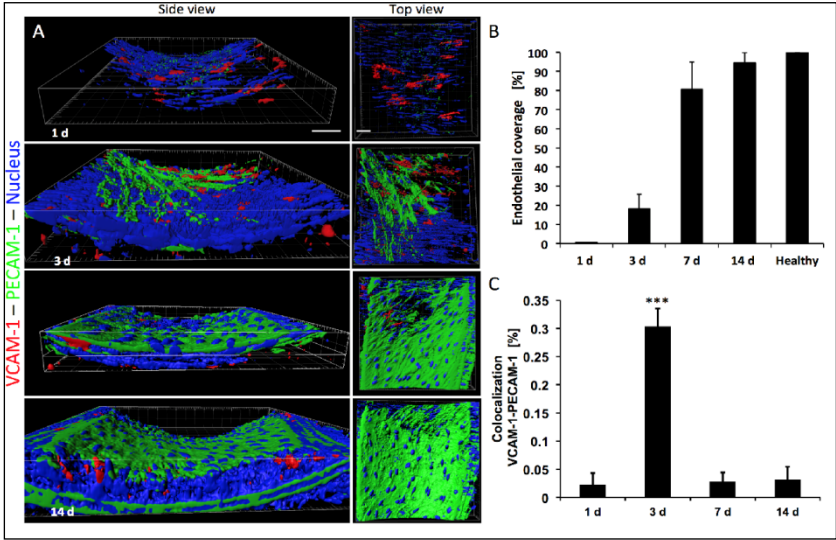
TPLSM images: ,The degree of endothelial regeneration, B,Percentage of endothelial coverage, C,availability of endothelial VCAM-1

Notes

POSTER PRESENTATIONS

POSTER #1

MAGNETOCARDIOGRAPHY (MCG) IMAGING WITH AN OPTICALLY PUMPED 4HE MAGNETOMETER AT ROOM TEMPERATURE

Labyt, E.[1], Morales, S.[2], Corsi, M. C.[2], Le Prado, M.[2], Berger, F.[1], Vanzetto, G.[3]

[1]CEA Clinatec, 17 rue des Martyrs, 38054 Grenoble, France ; [2]CEA DSIS, 17 rue des Martyrs, 38054 Grenoble, France ; [3]CHU Grenoble Urgences & Soins Intensifs Cardiologiques – INSERM U1039 Clinique Universitaire de Cardiologie CHU de Grenoble CS 10217, 38043 Grenoble, France

(etienne.labyt@cea.fr)

Introduction: Recently, several clinical studies have reported the interest of MCG in the diagnosis of coronary disease and cardiac arrhythmia (Agarwal et al. 2012; Fenici et al. 2013; Kwong et al. 2013). Despite this statement and the clinical need, MCG imaging, currently based on SQUIDs sensors, has never spread in cardiology practices, due to its high running cost and huge technical constraints.

Methods: Optically pumped 4He magnetometers (OPM) working at room temperature and requiring no running cost have been developed at CEA-LETI for cardiac imaging. At this step, a first clinical proof of concept of MCG recordings with one OPM, cross validated with ElectroCardioGram (ECG), has been performed in two healthy subjects. Recordings were carried out inside a magnetic shielded room.

Results: From real time OPM recordings, R peaks and T waves could be detected. Heart rate variability based on RR intervals was similar to ECG. After averaging, QRS complex and T wave can be obviously observed in our two subjects. QRS durations from ECG and MCG were not significantly different (t test, p = 0.1972).

Conclusions: This study revealed that our OPMs are able to record cardiac activity in healthy subjects at room temperature. Current efforts aim at building an OPM array to address MCG mapping issues and cardiac source reconstruction in order to localize pathological myocardia areas.

References: Agarwal, Rajender, Abhimanyu Saini, Tareq Alyousef, and Craig A. Umscheid. 2012. "Magnetocardiography for the Diagnosis of Coronary Artery Disease: A Systematic Review and Meta-Analysis." *Annals of Noninvasive Electrocardiology: The Official Journal of the International Society for Holter and Noninvasive Electrocardiology, Inc* 17 (4): 291–98. Fenici, R., D. Brisinda, A. Venuti, and A. R. Sorbo. 2013. "Thirty Years of Clinical Magnetocardiography at the Catholic University of Rome: Diagnostic Value and New Perspectives for the Treatment of Cardiac Arrhythmias." *International Journal of Cardiology* 168 (5): 5113–15. Kwong, Joey S. W., Boris Leithäuser, Jai-Wun Park, and Cheuk-Man Yu. 2013. "Diagnostic Value of Magnetocardiography in Coronary Artery Disease and Cardiac Arrhythmias: A Review of Clinical Data." *International Journal of Cardiology* 167 (5): 1835–42.
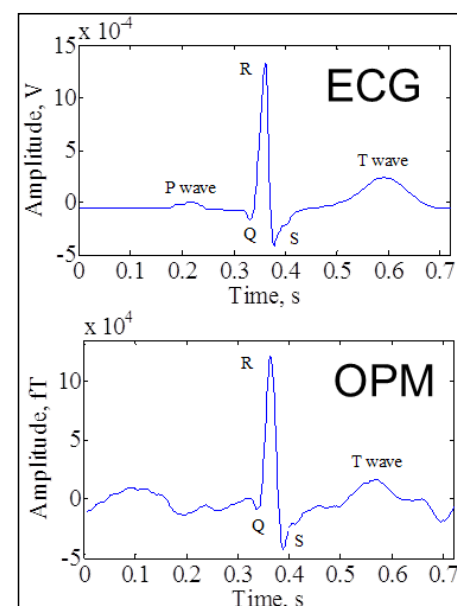
Comparison ECG / MCG: Comparison of averaged data from ECG and MCG recorded with 4He optically pumped magnetometer (OPM)
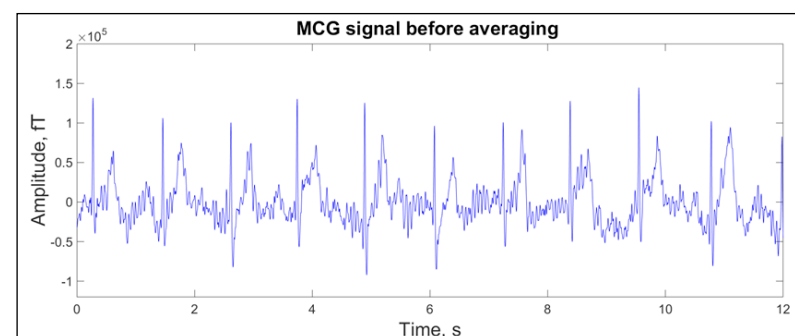
Real time MCG recording: Real time MCG recording on which R peaks and T waves can be detected

POSTER #2

ASSESSMENT OF THE RELEVANCE OF DIFFERENT IMAGE-DERIVED PARAMETERS FOR THE DESCRIPTION OF MYOCARDIAL VIABILITY AFTER ACUTE MYOCARDIAL INFARCTION

Viel, T.[1,2], Lemarié, J.[1,3,4], Ait-oufella, H.[1,5], Tavitian, B.[1,2,6]

[1]INSERM PARCC-U970, 56 rue Leblanc, 75015 Paris, France ; [2]Université Paris Descartes UFR de Médecine, Paris, France ; [3]INSERM - Université de Lorraine UMR S1116, Nancy, France ; [4]CHU de Nancy Medical Intensive Care Unit, Nancy, France ; [5]Assistance Publique-Hôpitaux de Paris Hôpital Saint-Antoine, Paris, France ; [6]Assistance Publique-Hôpitaux de Paris Hôpital Européen George Pompidou, Paris, France

(thomas.viel@inserm.fr)

Introduction: Acute myocardial infarction (AMI) is the cause of 12% of total deaths worldwide and is associated with high morbidity rates. Non-invasive imaging of AMI aims to explore disease-specific processes and potential therapeutic targets. PET imaging of cardiac FDG uptake has been shown to measure myocardial viability in Humans and large animals, but remains challenging in mice although this is the most frequently used animal model. We have performed sequential cardiac PET imaging in a mouse model of AMI with the aim to obtain image-based parameters describing myocardial viability.

Methods: A thoracotomy was performed in C57Bl6 mice and the left coronary artery was permanently ligated at its site of emergence under the left atrium. FDG-PET images were acquired 2, 7 and 15 days after infarction in a nanoScan PET/CT (Mediso Ltd., Hungary). FDG (10 MBq in 0.2 mL saline) was injected into the tail vein under anesthesia with 2% isoflurane in 100% O_2. Body temperature, respiration and ECG were registered and the animals were maintained at 36°C during the entire procedure. List-mode PET data were collected between 30 and 60 min post injection and sorted into 8 frames of equal duration with ECG triggering. Images were analyzed using automatic segmentation with the PMOD software (PMOD Technologies, Switzerland). A spherical VOI covering the heart was drawn during the systolic and the diastolic frames.

Results: At the time of submission of the present abstract, we have analyzed results from 4 mice at days 2, 7 and 15 post AMI. SUV in VOIs defined by pixels with uptake higher than 50% of the 10 hottest pixels yield reproducible measurements of FDG uptake. Max and mean SUV are 21% higher for the systolic than for diastolic time frames. From day 2 to day 15 post-AMI, max and mean SUV increase by 10% and 23% for the systolic and the diastolic frames, respectively, and metabolic volumes (Mean SUV * VOI volume) increase by 53% and 30% for the systolic and diastolic frames, respectively. We will now compare diastolic and systolic time-frame measurements, together as well as with non-gated image reconstructions, increase the number of animals and compare image-derived parameters with histology. Furthermore, polar map analysis will be performed using the *Cardiac* Modeling Tool of the PMOD software (Zürich, Switzerland).

Conclusions: Our preliminary results indicate that quantitative measurements of myocardial viability after AMI in mice using non-invasive FDG-PET may be feasible. Additional analysis will be performed and further validated in order to identify robust and accurate methods for quantitative analysis of cardiac PET image in mice.

POSTER #3

MAPPING MYOCARDIAL FIBER ORIENTATION USING ULTRASOUND BACKSCATTER TENSOR IMAGING

Papadacci, C., Finel, V., Provost, J., Tanter, M., Pernot, M.

Institut Langevin, ESPCI ParisTech, CNRS UMR 7587, INSERM U979, Université Paris 7 Paris, 4, rue Jussieu, 75005 Paris, France

(victor.finel@espci.fr)

Introduction: The orientation of myocardial fibers is linked to the mechanical and electrical properties of the heart and its assessment is of great interest to better understand the progression of myocardial disease. Yet there is no clinical imaging modality to map the myocardial fiber orientation routinely. In this study, we present Backscatter Tensor Imaging (BTI), a novel 3D ultrasound-based technique that can map the myocardial fibers by analyzing the spatial coherence of backscattered echoes. Application in phantoms and *ex-vivo* muscles will be shown.

Methods: Acquisitions were performed using a 2D matrix array (3 MHz, 32x32 elements, 0.3-mm pitch) driven by a customized, programmable, 1024-channel ultrasound system in phantoms, and in *ex-vivo* and in-vivo muscle tissue. Up to 81 tilted 3D plane waves were emitted and coherently compounded to focus in each voxel of the volume. The coherence of the signals recorded by each element of the probe was calculated as described in Figure 1 (from [1]) for each focal zone and an elliptic fit was used to identify the local fiber orientation.

Results: The isotropic phantom was used to verify the Van Cittert Zernike theorem, which predicts that if the medium is isotropic, the coherence function will only be impacted by the geometry of the probe. 3D BTI was then applied in phantoms and *ex-vivo* muscles, which were found to be approximately orthotropic (Figure 2).

Conclusions: 3D BTI was successfully applied to the in vitro and ex vivo muscle. These results suggest that 3D BTI could be used for in vivo applications, as the technique can be applied with high frame rates. Its application in the human heart in-vivo is the subject of ongoing work.

References: [1] Clement Papadacci. Imagerie échographique ultrarapide du cœur et des artères chez l'homme : Vers l'imagerie ultrarapide 3D et l'imagerie du tenseur de retrodiffusion ultra-sonore. Medical Physics. Universite Paris-Diderot Paris 7, 2014. French.
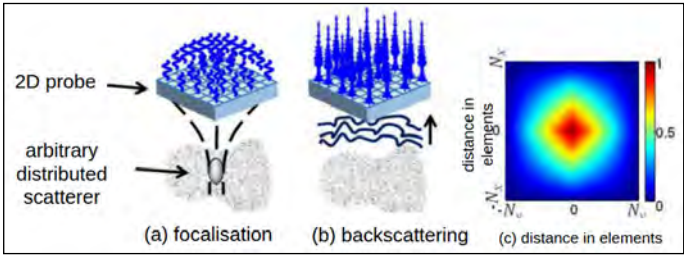
Figure 1: Principle of spatial coherence with a 2D matrix probe. (a) A wave is focalised in a medium. (b) Backscattered signals are recorded. (c) Theoretical coherence function for randomly distributed scatterers in the medium, imaged with a NX*NX elements probe.
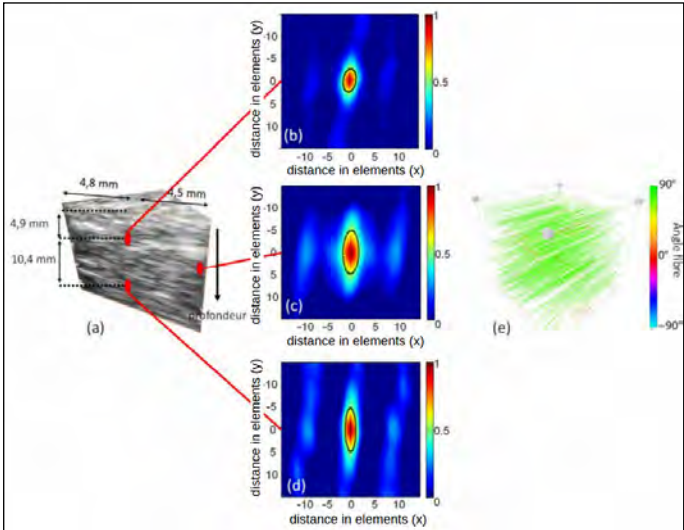

Figure 2: (a). B-mode imaging of a muscle. (b),(c),(d) : coherence function is estimated on 3 points of the volume. The ellipses give the direction of the fibers. (e) 3D vectorial representation of the fibers.

POSTER #4

HYALURONIC ACID: ANTI-ANGIOGENIC SHIELD FOR THE EARLY EMBRYO

Hadas, R.[1], Gershon, E.[2], Cohen, A.[1], Lazar, S.[3], Atrakchi, O.[1], Eilam-Altstadter, R.[4], Dekel, N.[1], Neeman, M.[1]

[1]The Weizmann Institute of Science Biological Regulation, Herzl 234, Rehovot, Israel ; [2]Agricultural Research Organization, Volcani Center Department of Ruminant Science, 50250 Bet-Dagan, Israel ; [3]Institute for Biological Research, 7410001 Ness-Ziona, Israel ; [4]The Weizmann Institute of Science Department of Veterinary Resources, Herzl 234, Rehovot, Israel

(ron.hadas@weizmann.ac.il)

Introduction: Embryo implantation, a critical step in the establishment of pregnancy, is immediately followed by a marked increase in the permeability of the uterine blood vessels. Hyaluronic acid (HA) has been reported to participate in the regulation of vascular de-velopment in a number of physiological processes. Specifically, high molecular weight HA has been shown to inhibit angiogenesis, whereas its enzymatic degradation products are pro-angiogenic. On the basis of this information, we hypothesized that HA is involved in vascular modifications associated with implantation. Our experiments revealed that HA deposition and degradation correlates with vascular remodeling in the implantation site during early pregnancy.

Methods: Moreover, extensive changes in the distribution of HA synthesis and degrading enzymes were observed during implanta-tion by use of immunohistochemistry. In addition, in-vivo MRI of pregnant mice allowed detection of embryo implanatation sites and assesment of their vasculature functionality. Furthermore, by means of whole tissue clarity method, maternal blood vessels, tissue macrophages and the embryo, were visualized by confocal microscopy.

Results: Functional MRI inspection of pregnant mice, carrying embryos, the trophoblast cells of which over-express HA degrading en-zyme, showed defective implantation. Specifically, an increased permeability of blood vessels surrounding the embryo accompanied by infiltration of endothelial cells ultimately resulted in multiple embryo resorptions. In addition, immuno-labeling of cleared embryo implan-tation sites, enabled detection of immense macrophage infiltration to the embryonic niche as a result of Hyaluronidase over-expression. Interestingly, over-expression of HA synthesizing enzyme, in trophoblast cells, resulted in the termination of pregnancy associated with an opposite phenotype, i.e, reduced permeability of blood vessels in the embryonic niche and a decrease in fractional blood volume.

Conclusions: Taking these observations into account, we suggest that HA uterine metabolism has a pivotal role in vascular remodeling essential for successful embryo implantation in mice. Our study sheds light on the participation of the extracellular matrix in the complex chain of vascular events involved in successful pregnancy, thus deciphering new components responsible for gestational disturbances.
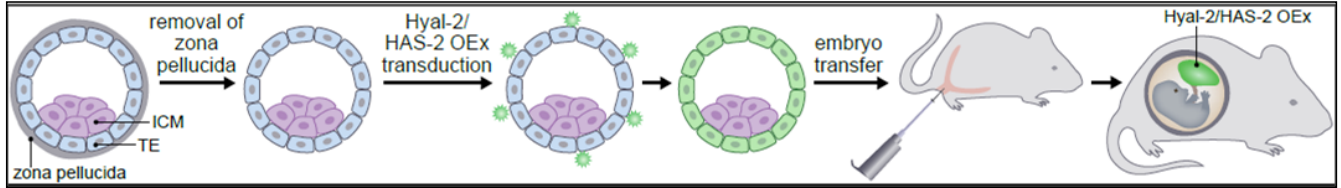

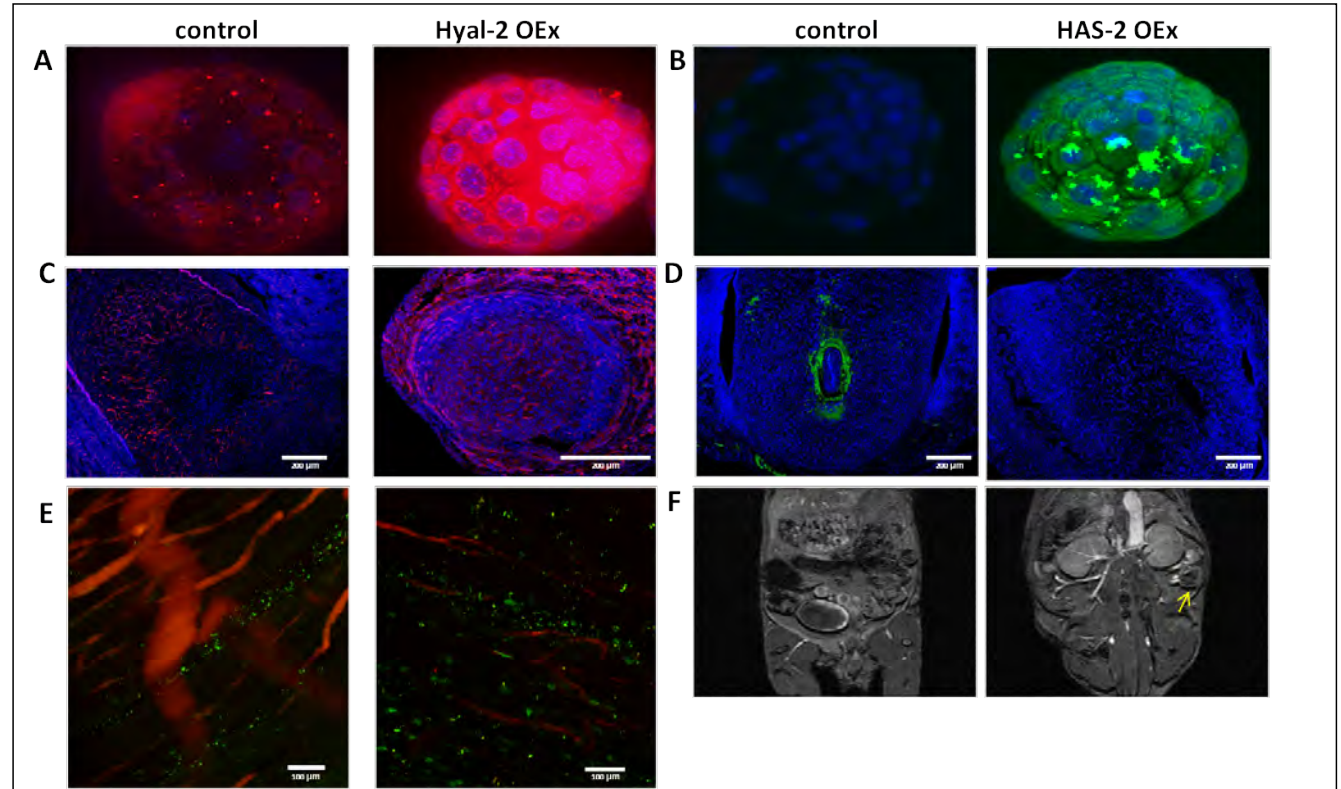Figure1: Trophoblast-specific lentiviral gene transfer

Figure 2. Maintenance of HA balance is essential for embryo implantation. (A,B) Hyal-2 and HAS-2 were over expressed in Blastocysts' trophoblast cells. Representative images of whole-mount immuno-fluorescence for Hyal-2 in blastocysts following lenti-viral transduction. (C) Ectopic presence of newly formed blood vessels in the embryonic niche was observed in the Hyal-2 OEx group, as opposed to the control group; CD34 in red. (D) Visualization of hyper-permeable blood vessels in the embryonic niche was conducted by staining of, biotin-BSA-GdDTPA, 40 minutes after i.v injection; biotin-BSA-GdDTPA in green. (E) Macrophage infiltration to the embryonic niche was demonstrated using immuno-staining of macrophages in implantation sites harvested from surrogate mothers injected with ROX labeled lectin.; mac-2 in green (F) GE T1 weighted images of embryo implantation sites, acquired from pregnant mice at E6.5 30 minutes after administration of biotin-BSA-GdDTPA. Little accumulation of biotin-BSA-GdDTPA was observed in the HAS-2 OEx group in comparison to the control group.

Figure2: Balanced HA metabolism is essential for embryo implantation

POSTER #5

DENDRITIC B-ADRENERGIC BINDING LIGANDS FOR EARLY DETECTION OF HEART FAILURE BY PET-IMAGING

Böhmer, V. I.[1,2], Elzes, M. R.[1], Slart, R. H. J. A.[2,3], Elsinga, P. H.[2], Paulusse, J. M. J.[1,2]

[1]University of Twente Biomaterials Science and Technology, Drienerlolaan 5, 7522 NB Enschede, Netherlands; [2]University Hospital Centrum Groningen Nuclear Medicine and Molecular Imaging, Hanzeplein 1, 9713 GZ Groningen, Netherlands; [3]University of Twente Biomedical Photonic Imaging, Drienerlolaan 5, 7522 NB Enschede, Netherlands

(p.h.elsinga@umcg.nl)

Introduction: Nuclear imaging can be used for qualitative and quantitative assessment of cardiac autonomic function in patients with (early) heart failure. Abnormal β_1-adrenoceptor (β_1-AR) signalling of the failing heart is related to a lowered β_1-AR density on the myocardium which can be evaluated by non-invasive positron emission tomography (PET) imaging. Successful development of a selective β_1-AR binding ligand (β_1-AR ligand) has so far not been established. Hence, a novel strategy has been chosen based on multivalency to increase the binding affinity (BA). It was shown for the ligand esmolol that bivalent interactions are able to remark-ably enhance BA. The aim of the current study is the synthesis of ^{18}F-labelled dendritic β_1-AR ligand with an attractive half-life of 110 minutes for PET-imaging.

Methods: The strategy for the dendritic ligand synthesis is based on the ^{18}F-labelling method using the alkyne-azide click reaction. The following three step synthesis shown in Figure 1 was carried out:

1. Synthesis and characterization of multivalent binding ligands
Poly(amido amine)-based dendrimers (PAMAMs) were synthesized using two different cores, namely 1,7-octadiyne and ethylenediamine followed by alternating photo-initiated thiol-yne click reactions and *aza*-Michael additions.

2. Functionalization with β_1-AR ligands
β_1-AR ligands, i.e. commercially available β-blockers, have been modified with thiol-functionality, which subsequently can be coupled to the alkyne-surface through a thiol-yne click reaction. Monovalent ligand synthesis was based on a thiol-ene Michael-addition.

3. ^{18}F-labelling
Results: The β_1-AR antagonist alprenolol was successfully modified. PAMAM dendrimers were prepared and characterized. These were employed in the formation of hexavalent binding ligands, functionalized with β_1-AR ligands. Dendrimers were already used in nuclear imaging, but this novel dendrimer enables the synthesis of a tuneable valency ligand in minimal reaction steps. The resulting alkyne surfaces can simply be functionalized with β_1-AR ligand and ^{18}F using click-chemistry.

Conclusions: A novel dendrimer synthesis was developed to prepare multivalent β_1-AR imaging agents that achieve branching in each reaction step with tuneable multivalency of alkyne surfaces. Different β_1-AR ligands will be tested for BA and radio-labelling with [18]F.
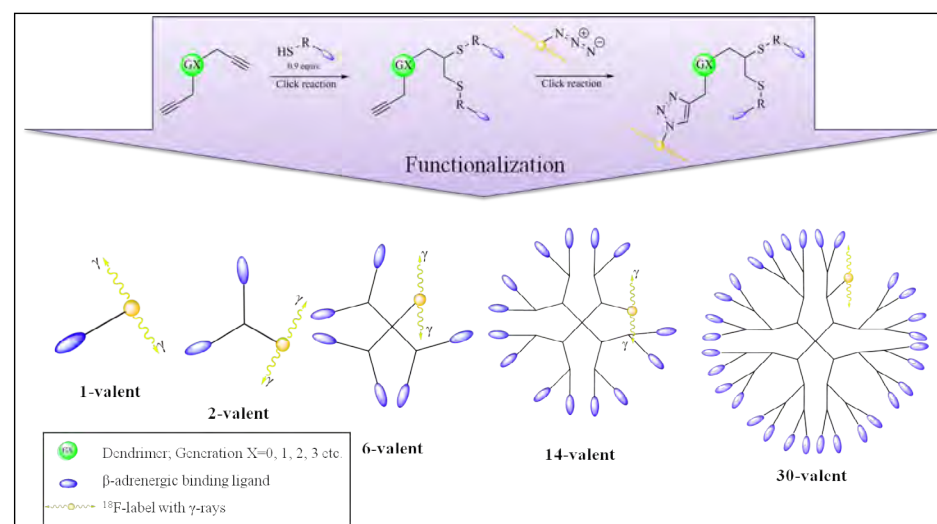

Figure 1.: Synthesis process of an improved PET-tracer for β1-AR imaging

POSTER #6

SERIAL FDG-PET/CT REVEALS RESOLUTION OF DIET-INDUCED INFLAMMATION IN LATE STAGE ATHEROSCLEROTIC PLAQUES IN APOE-/- MOUSE

Xing, X., Kloth, C., Hermann, S., Schäfers, M.

European Institute for Molecular Imaging – EIMI Westfälische Wilhelms-Universität Münster, Waldeyerstraße 15, 48149 Münster, Germany

(xinx@uni-muenster.de)

Introduction: Imaging of inflammatory activity of atherosclerotic plaque is thought to identify vulnerable and life threatening lesions prone to rupture. Assessing increased uptake of ^{18}F-FDG by macrophages using PET/CT has been shown to be a promising imaging strategy. However, the individual time course of the inflammatory activity in the ApoE-/- mouse model of atherosclerosis is not fully investigated. Aim of this study was the longitudinal monitoring of inflammatory activity of plaque lesions in the aorta of individual ApoE-/- mouse.

Methods: Formation of atherosclerotic plaques in ApoE -/- mice (age~12weeks) was induced by a high fat and cholesterol-rich diet (HFC, 15.8% fat, 1.25% cholesterol). Serial ^{18}F-FDG-PET/CTs were performed before as well as 4, 6, 8, 10 and 12 weeks after onset of diets. FDG uptake was quantified in CT-defined segments of the aorta. Regional FDG uptake in the aorta is expressed as plaque/background ratio (P/B) using the vena cava as background region of interest. Blood samples were taken at all time points for analysis of white blood cells (WBC). Subsequent to the week 12 PET/CT, the aorta was explanted and analyzed by histology and immunohistochemistry.

Results: Under HFC diet ApoE-/- mice developed varying degrees of atherosclerotic plaques as determined at week 12. While in the baseline scan no significant aortic FDG uptake was observed (P/B < 2), all ApoE-/- mice presented with increased FDG accumulation in the aorta during the course of the disease. Surprisingly, after an initial increase the FDG uptake peaked 8 weeks (P/B: 3.2) after onset of the aggressive HFC diet and declined thereafter until the final measurement by 28% (P/B: 2.3). In addition, the FDG uptake still peaked at 8weeks (P/B increased to 7.6) and P/B declined 24% to 5.8 at 12weeks after changing the fasting time from 18h to 10h. While the time course of WBC showed a significant increase preceding the peak of FDG uptake and stabilizing thereafter.

Conclusions: ^{18}F-FDG-PET/CT can be applied in ApoE-/- to quantitatively assess the time course of inflammatory plaque activity in the aorta. As expected, HFC diet leads to an initial increase in aortic FDG uptake with a further increase under shorter fasting time condition. However, FDG uptake dropped significantly after reaching an initial peak, which could point to a resolution phase of inflammation in later stage plaques in ApoE-/- mouse. Further studies are mandatory to investigate the observed biphasic time course of plaque inflammation.

POSTER #7

GLUCOSE METABOLISM IMAGING OF ANTI-ANGIOGENIC RELATED CARDIOTOXICITY

Sourdon, J.[1,2], Viel, T.[1,2], Balvay, D.[1,2], Lager, F.[3,2], Renault, G.[3,2], Tavitian, B.[1,2,4]

[1]INSERM U970 - Paris Centre de Recherche Cardiovasculaire (PARCC), 56 rue Leblanc, 75015 Paris, France ; [2]Université Paris Descartes - Sorbonne Paris Cité, Paris, France ; [3]INSERM U1016 - Institut Cochin, Paris, France ; [4]Hôpital Européen George Pompidou, Assistance Publique-Hôpitaux de Paris (AP-HP) Service de radiologie, Paris, France
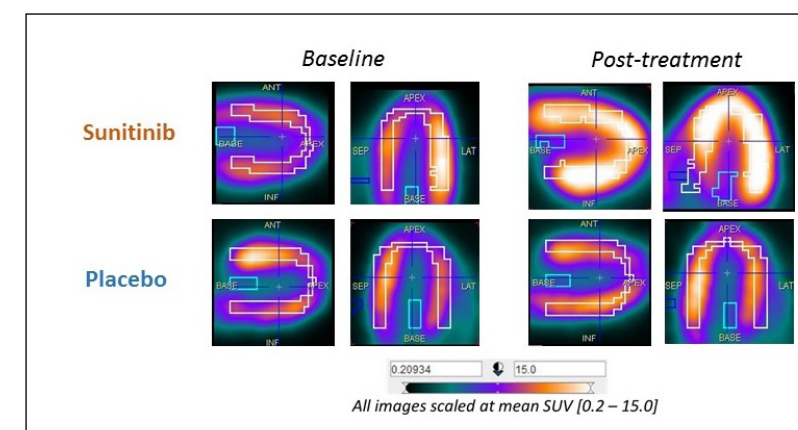
(joevin.sourdon@inserm.fr)

Introduction: Angiogenesis is a major event during tumor development and anti-angiogenic treatments are administered to prevent tumor development by blocking the formation of neo-vessels. In some cases, drugs targeting angiogenesis may induce severe systemic side effects such as impaired heart function and hypertension. During the course of a PET imaging study using the multi-targeted receptor tyrosine kinase inhibitor sunitinib in tumorized nude mice, we serendipitously observed an increase in 2-deoxy-2[^{18}F]fluoro-D-glucose ([18]FDG) uptake in the myocardium. Here, we explore this surprising observation about the effect of sunitinib on [18]FDG uptake in the myocardium.

Methods: Four groups of mice aged 17 – 20 weeks were compared: (i) nude mice treated with sunitinib 50 mg.kg^{-1} (n=9), (ii) nude mice treated with placebo (DMSO + PBS) (n=6), (iii) C57Bl6 mice treated with sunitinib 50 mg.kg^{-1} (n=6) and (iv) C57Bl6 mice treated with placebo (n=6). Mice were fasted and a baseline PET was acquired during 60 min after tail vein injection of 10 MBq [18]FDG in a nanoScan PET-CT camera (Mediso, Hungary). Then, mice received treatments by gavage during 5 days, followed at day 7 by a post-treatment PET-CT. Whole body and heart FDG images acquired were analyzed using PMOD software with Standardized Uptake Value (SUV) calculation. C57Bl6 mice were also explored at baseline and post-treatment by echocardiography in a Vevo 2100 (VisualSonics, Canada).

Results: Compared to baseline, SUV was increased by 50 ±13 percent in nude mice treated with sunitinib (p=0.0003) while it increased only by 17±26 percent in the placebo-treated group (n.s). In the sunitinib group, Patlak analysis showed an increase of 57±11 percent of the slope (representing glucose influx) in the myocardium compared to baseline (p=0.002), while this parameter remained unchanged in the placebo group.

Results were similar in C57Bl6 mice: compared to baseline, myocardial SUV increased by 44±30 percent in sunitinib-treated mice (p=0.04) and by 16±47 percent in the placebo group (n.s). Moreover, sunitinib-treated mice showed a dramatic reduction of cardiac output (product of heart rate by stroke volume) by 59±36 percent (p=0.01) while in contrast in placebo-treated mice there was a slight increase of 13±22 percent (n.s).

Conclusions: In conclusion, FDG PET-CT imaging shows that [18]FDG uptake is dramatically increased by sunitinib treatment. These data suggest that sunitinib treatment is associated with a major metabolic dysregulation in the heart that may contribute to impairing cardiac function and could result, either from a direct action of the drug on the heart, or from its action on other organs and peripheral vessels.

FDG images of myocardium: Uptake of FDG in mouse myocardium 45-60 min after administration. Same color scale [SUV = 0.2 - SUV = 15] for all panels. Top: sunitinib-treated mouse, Bottom: placebo-treated mouse, Left: baseline PET, Right: post-treatment PET.

POSTER #8

FEMORAL ARTERY CUFF IMPLANTATION: A NEW MODEL OF PERIPHERAL SHEAR STRESS INDUCED ATHEROSCLEROSIS

Eligehausen, S.[1], Kuhlmann, M.[1], Hermann, S.[1], Schäfers, M.[1,2]

[1]University of Muenster European Institute for Molecular Imaging, 48149 Münster, Germany ; [2]University Hospital Muenster Department of Nuclear Medicine, 48149 Münster, Germany

(selig_01@uni-muenster.de)

Introduction: Modifications of vascular shear stress have been reported to trigger the development of atherosclerotic lesions. We have recently developed a mouse model in which a shear stress modifying cuff implanted around the common carotid artery leads to phenotypically distinct atherosclerotic lesions up- and downstream of the cuff [1]. To investigate whether plaque development in the peripheral vascular system is similar to that in the carotid artery, we aimed to transfer the carotid cuff model to the femoral artery. We compared the modification of shear stress at the two locations using ultrasound, and the development of atherosclerotic lesions by optical imaging of MMP2/9 activity as well as subsequent histology. Mimicking the clinical situation of the peripheral artery disease, this model will help to get better insight into the development of the disease.

Methods: ApoE-KO mice (n=6) were fed a high fat, high cholesterol diet. 4 weeks after the start of the diet, a shear stress modifying cuff was placed around the right common carotid artery and a second one around the left femoral artery. Non-operated arteries served as controls in all measurements. Shear stress was measured by ultrasound after cuff implantation. 8 weeks post surgery, mice received 2nmol of Cy5.5-AF443 targeting MMP2/9. Fluorescent reflectance imaging (FRI) was performed 4h p.i.. Sections of the carotid and femoral artery up- and downstream of the cuff were histological stained with HE, Mac-3 and MRP-14.

Results: Ultrasound measurements after cuff implantation showed comparable shear stress modifications at the femoral cuff (FC) with those at the carotid cuff (CC). Plaques were detectable by increased MMP2/9 activity by FRI 8 weeks after surgery at the FC (Rad. Eff. (x10^7) cuff: 4.1±1.0 vs control 1.4±0.1), and at the CC (Rad. Eff.(x10^7) cuff: 7.14±1.1 vs control 4.56±0.4). Histological stainings confirmed plaque development up- and downstream of the FC and CC. We are currently investigating whether the phenotype of plaques up- and downstream of the FC correlate with regional flow dynamics, as we previously described for the CC.

Conclusions: For the first time, we report the development of a mouse model of atherosclerosis with defined atherosclerotic lesions in the peripheral vascular system by placing a shear stress modifier around the femoral artery. This new model closely mimics the clinical situation of peripheral artery disease. Additionally, the superficial location of the lesions make it a promising candidate for optical imaging techniques like FRI and 2-Photon-Microscopy.

References: [1] Kuhlmann et al. 2012, Implantation of a carotid cuff for triggering shear-stress induced atherosclerosis in mice, J Vis Exp

POSTER #9

SPECKLE-TRACKING BASED STRAIN AND STRAIN RATE ECHOCARDIOGRAPHY IN EXPERIMENTAL PRESSURE OVERLOAD-INDUCED RIGHT VENTRICULAR HYPERTROPHY

Kojonazarov, B.[1], Boehm, M.[1], Novoyatleva, T.[1], Lu, C.[1], Grimminger, F.[1], Ghofrani, H. A.[1], Weissmann, N.[1], Seeger, W.[1,2], Schermuly, R.[1]

[1]Universities of Giessen and Marburg Lung Center, Aulweg, 130, 35390 Giessen, Germany ; [2]Max Planck Institute for Heart and Lung Research, Bad Nauheim, Germany

(baktybek.kojonazarov@innere.med.uni-giessen.de)

Introduction: Although, the prevalence of left ventricular (LV) dysfunction as a result of right ventricular (RV) pressure overload is extensively discussed, to date there have been no data showing speckle-tracking imaging (STI) based analysis of LV function in experimental pressure overload-induced RV hypertrophy. The objective of the present study was to investigate LV function in mice with pressure overload-induced RV hypertrophy and failure by conventional and STI-based echocardiography and its relationship with RV function

Methods: RV pressure overload was produced in mice by surgical pulmonary artery banding (PAB). Twenty-one days after surgery, standard echocardiographic examination in PAB and sham operated mice by Vevo2100 (Visualsonics, Canada) were performed to measure right (RV) and left ventricular (LV) structure and function. Parasternal long-axis view was used for STI based longitudinal strain (LS) and strain rate (LSR) analyses of interventricular septum (IVS) and LV wall (LVW) in mice. Whereas parasternal short-axis view (at the mid-papillary level) was obtained for circumferential strain (CS) and strain rate (CSR), radial strain (RS) and strain rate (RSR) analyses. Right heart catheterization were performed.

Results: Conventional echocardiography demonstrates that PAB caused a significant RV dilatation and hypertrophy accompanied by RV systolic and diastolic dysfunction. Speckle tracking based echocardiographic analyses demonstrate that PAB mice in comparison with sham-operated animals had significantly reduced LVW LS (-16.55±2.98 versus -22.76±5.51%; p<0.05) and IVS LS (-13.66±2.02

versus 19.71±2.76%; p<0.001). However, both LVW LSR and IVS LSR were not significantly altered in PAB mice in comparison with sham control. Our data revealed that PAB mice had significantly reduced IVS RS (p<0.01) and IVS CS (p<0.01) in comparison with sham mice. However, LVW RS and LVW CS were not significantly change compared with sham-operated animals, suggesting preserved LVW systolic function at the level of mesocardium. Additionally, both RSR and CSR in IVS and LVW in PAB animals were not significantly changed in comparison with sham control suggesting preserved contractility of the IVS and LVW.

Conclusions: Our data demonstrates that pressure overload leads to deterioration of the LV longitudinal systolic deformation and further impairs circumferential and radial strain in IVS. We also report that despite impairment of LV systolic function analyzed by strain and conventional echocardiography, the LV LSR, CSR and RSR were not altered in PAB animals in comparison with sham control, suggesting compensated LV contractility.

POSTER #10

MESENCHYMAL STEM CELL-LOADED TISSUE-ENGINEERED PATCHES ACT AS A RESERVOIR OF PARACRINE FACTORS IN MYOCARDIAL INFARCTION

Blondiaux, E.[1,2], Autret, G.[1,3], Pidial, L.[1], Balvay, D.[1,3], Wilhelm, C.[4], Menasché, P.[1,5], Clément, O.[1,6]

[1]Paris Cardiovascular Research Center, INSERM U970, Université Paris Descartes, Sorbonne Paris Cité, 56 rue Leblanc, 75015 Paris, France ; [2]Radiology Department, Assistance Publique - Hôpitaux de Paris, Hôpital Trousseau, Université Pierre et Marie Curie, 26 avenue du Docteur Arnold-Netter, 75012 Paris, France ; [3]Plateforme Imageries du Vivant, Université Paris Descartes, Sorbonne Paris Cité, 56 rue Leblanc, 75015 Paris, France ; [4]Laboratoire Matière et Systèmes Complexes, UMR 7057 CNRS, Université Paris-Diderot, 10 rue Alice Domon et Léonie Duquet - Bâtiment Condorcet, 75205 Paris cedex 13, France ; [5]Department of Cardiovascular Surgery, Assistance Publique - Hôpitaux de Paris, Hôpital Européen Georges Pompidou, 20 rue Leblanc, 75015 Paris, France ; [6]Department of Radiology, Assistance Publique - Hôpitaux de Paris, Hôpital Européen Georges Pompidou, 20 rue Leblanc, 75015 Paris, France
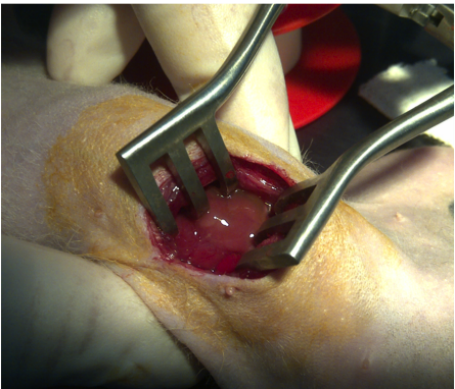
(gwennhael.autret@inserm.fr)

Introduction: To determine whether the efficiency of epicardial deposit of human bone marrow-derived mesenchymal stem cells (BMSC) fibrin patch on chronically infarcted rat hearts occurred through integration of stem cells from the patch to the recipient myocardium.

Methods: BMSC were labeled with iron oxide nanoparticles (BMSC*, n=12) or unlabeled (BMSC-, n=10). Patches were applied to region of ischemia. No patch was applied to control group hearts after myocardial infarction and median sternotomy (SHAM, n=7). In vivo cardiac MR imaging was performed on a 4.7 Tesla scanner before, 8 days and 21 days after transplantation. Therapeutic efficacy was evaluated on cine flash MRI sequences with left ventricular ejection fraction (LVEF). Cell migration into the myocardium was evaluated on in vivo T2*-weighted sequences. The results were compared with histology for the evaluation of iron labeled cells (Perls) and immunohistochemistry for the presence of human cells (Lamin A/C).

Results: At day 8 and 21 after transplantation, a statistically significant difference was found between the LVEF of BMSC* and BMSC- compared with SHAM (p=0.02 and p=0.03 respectively). Persisting human cells were identified in the grafted area 21 days after transplantation. Location of dark areas identified on T2*-weighted MR images corresponded with spatially MR-matched histological sections and demonstrated that no BMSC* integrated in the myocardium.

Conclusions: The absence of integration BMSC into the recipient myocardium and the presence of persisting human cells at day 21 suggest that the efficiency of these constructs is more closely related to the paracrine effects of BMSCs.

Patch: Epicardial deposit of human bone marrow-derived mesenchymal stem cells (BMSC) fibrin patch

GE T2* cardio MRI at D21   Perls coloration   Immunofluorescence
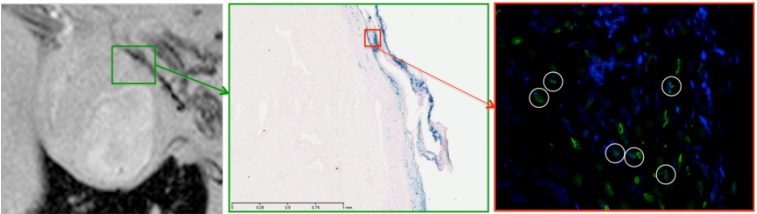
Patch Detection: Patch and BMSC detection by MRI (T2*), Perls coloration and immunofluorescence

POSTER #11

NONINVASIVE MONITORING OF POST-INTERVENTIONAL IN-STENT REGENERATION

Wu, Z.[1,2], Curaj-Baleanu, A.[2], Kiessling, F.[2], Liehn, E.[1]

[1]RWTH-Aachen University Institute for Molecular Cardiovascular Research, Pauwelsstrasse 30, 52072 Aachen, Germany ; [2]RWTH-Aachen University Institute for Experimental Molecular Imaging, Pauwelsstrasse 30, 52072 Aachen, Germany

(zwu@ukaachen.de)

Introduction: With the introduction of balloon angioplasty into clinical routine, mortality rates of coronary stenosis and acute myocardial infarction have drastically decreased. A major factor for the improvement of cardiovascular intervention was also the combination with bare metal stents. However, revascularization procedures with stent implantation also induce severe damage to the vascular wall, leading to an inflammatory reaction and a high risk for thrombus formation and restenosis. Due to the inability of noninvasive clinical imaging modalities to penetrate conventional metal stents, complications can occur unexpectedly and deadly. Polyvinylidene fluorid (PVDF) is a biocompatible material which permits clinical imaging modalities to penetrate and will be used as a new stent material. In combination with Ultrasound, which is the most desirable imaging modality due to low costs and bedside availability it provide a great opportunity to monitor post-interventional recover. However, due to the lack of functional imaging capabilities of conventional US, microbubbles(MBs) as target specific contrast agents are needed for the detection of molecular markers.

Methods: C57BL/6 mice were subjected to stent implantation in the common carotid arteries. Molecular ultrasound imaging using VCAM-1 targeted MBs was performed at different time points after the intervention (1d, 3d, 7d, 2 weeks). Using deep tissue two-photon laser scanning microscopy, 3D projection of the stent architecture and tissue composition was visualized (Figure 1). PVDF also permits histological embedding and cutting (Figure 2). We used classical immunohistological analysis to characterize inflammational marker expression (MAC2, VCAM-1, CD31) was performed.

Results: Ultrasound imaging penetrated implanted PVDF stents without image artefacts. The injection of microbubbles was observed and detectable within the stent. By autofluorescence, the stent was also visible during two-photon microscopy characterization.

Conclusions: In this study, we have shown that small diameter PVDF stents are both feasible in production as well as during implantation. PVDF is a much better alternatives than bare metal for research purposes, which allows routine histology. Moreover, PVDF is penetrable by noninvasive imaging using clinical ultrasound as well as by near infrared light for deep tissue two-photon imaging, which promotes this model for the elucidation of in-stent tissue repair mechanics and also the assessment of drugs and therapeutics in small animals in vivo.
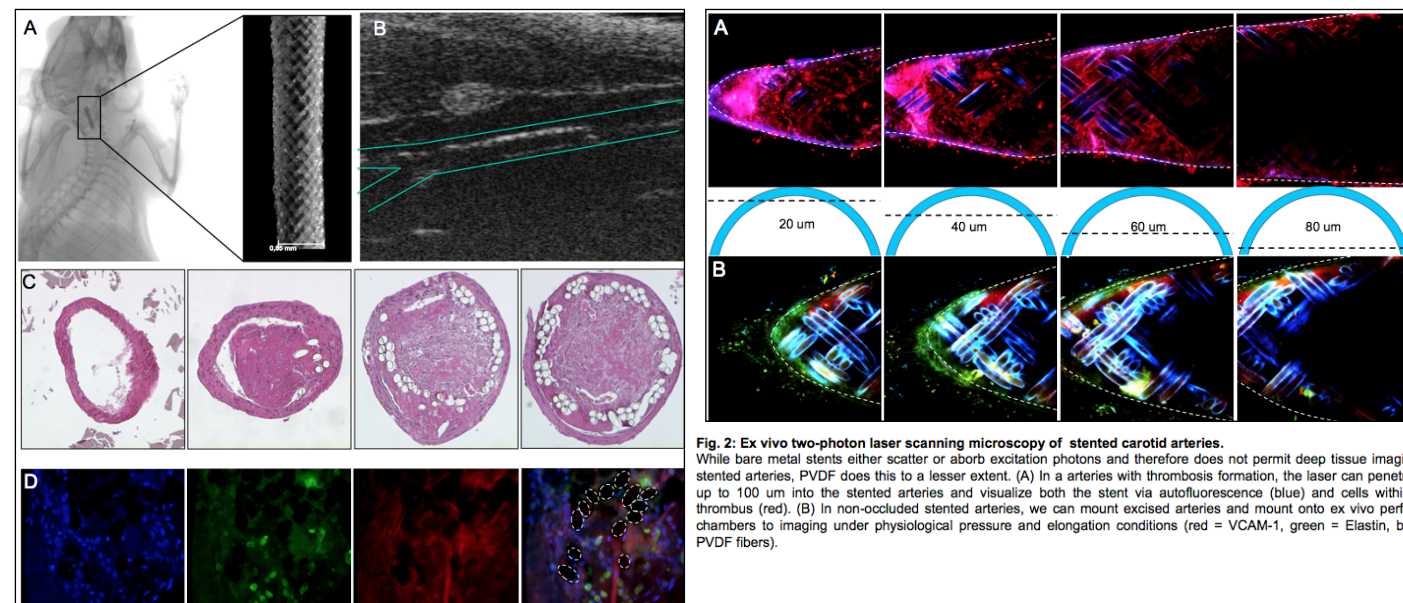

Fig. 2: Ex vivo two-photon laser scanning microscopy of stented carotid arteries.
While bare metal stents either scatter or aborb excitation photons and therefore does not permit deep tissue imaging of stented arteries, PVDF does this to a lesser extent. (A) In a arteries with thrombosis formation, the laser can penetration up to 100 um into the stented arteries and visualize both the stent via autofluorescence (blue) and cells within the thrombus (red). (B) In non-occluded stented arteries, we can mount excised arteries and mount onto ex vivo perfusion chambers to imaging under physiological pressure and elongation conditions (red = VCAM-1, green = Elastin, blue = PVDF fibers).

Fig. 1: In vivo stent imaging after implantation.
Implantation surgery have been established on bare metal stents, however imaging using CT was not possible penetrate the stent (A) Using molecular ultrasound on PVDF stents, it was possible to penetrate into the stent for potential molecular imaging, with no shadowing effects and imaging artefacts observed (B). Histological cuts of 5 um were done from thrombotized stents to investigate stent integrity and radial strength. (C) Immunohistological stainings of occluded carotid artery show thrombus composition (Dapi = Blue, MAC-2 = Green, SMA = Red. (D)

POSTER #12

IN VIVO IMAGING OF M2-MACROPHAGE RECRUITMENT AFTER MYOCARDIAL ISCHEMIA REPERFUSION INJURY IN RATS RECEIVING PPAR-GAMMA MODULATING AGENTS

Remory, I.[1,2], Donis, N.[3], Tierens, S.[1,2], Nguyen, T.[4], Bala, G.[5,2], Gillis, K.[5,2], Hernot, S.[2], Raes, G.[6,7], Cosyns, B.[5,2], Lahoutte, T.[8,2], Poelaert, J.[1]

[1]Universitair Ziekenhuis Brussel Department of Anaesthesiology, Laarbeeklaan 101, 1090 Jette, Belgium ; [2]Vrije Universiteit Brussel In Vivo Cellular and Molecular Imaging Lab, Laarbeeklaan 103, 1090 Jette, Belgium ; [3]Université de Liège GIGA, cardiovascular sciences, thrombosis and hemostasis laboratory, Avenue de l'Hopital 11, 4000 Liège, Belgium ; [4]Université de Lorraine École de Chirurgie, Faculté de Médecine, av Forêt de Haye ç, 54500 Vandoeuvre-lès-Nancy, France ; [5]Universitair Ziekenhuis Brussel Centrum voor Hart- en Vaatziekten, Laarbeeklaan 101, 1090 Jette, Belgium ; [6]Vrije Universiteit Brussel Laboratory of Cellular and Molecular Immunology (CIMM), pleinlaan 2, 1050 Brussel, Belgium ; [7]Vlaams Instituut voor Biotechnologie Laboratory of Myeloid Cell Immunology (MCI), Brussels, Belgium ; [8]Universitair Ziekenhuis Brussel Department of Nuclear Medicine, Laarbeeklaan 101, 19090 Jette, Belgium

(isabel.remory@gmail.com)

Introduction: Reperfusion of ischemic myocardium induces an inflammatory cascade. Initially, M1-macrophages, harboring a pro-inflammatory phenotype, are recruited. Subsequently, alternatively activated (M2) macrophages, harboring an anti-inflammatory phenotype, are responsible for healing and scar formation. The time-related presence of the different macrophage phenotypes is though to be of particular interest for prognosis and therapy. In a previous study we were able to show non-invasively the highest presence of CD206+ (M2) macrophages 5 to 9 days post IR injury.

We hypothesize that our *in vivo* imaging technique is sensitive enough to detect the PPARgamma-activator increased M2 macrophage subset in a rat model of myocardial IR injury. This promising technique allows following the impact of inflammation in acute ischemic heart disease.

Methods: 9-week-old Wistar rats (Charles River) (n=6) underwent coronary ligation surgery of the LAD artery; a temporary slipknot was made at the site of the LAD emergence from the left atrium. A sham-operated group (n=3) was included. Infarcted rats were randomly allocated into treatment groups, receiving 2,5mg/kg rosiglitazone (n=3), a PPAR-gamma agonist or 1mg/kg GW9662 (n=3), a PPAR-gamma antagonist IP for 9 days. Perfusion deficit was assessed on day 2 by a ^{99m}Tc-Tetrosomin scan. The recruitment of M2 macrophages in the infarcted area was imaged by pinhole-gated SPECT/CT (U-SPECT-II, MILabs, The Netherlands) using ^{99m}Tc-radiolabeled nanobodies (Nbs) targeting the macrophage mannose receptor (MMR, CD206+) (^{99m}Tc-MMR-Nb) at day 5, 7, 9, 12, 14 and 16.

Results: The perfusion percentage, was 40±28.2%, 58±1.2% and 95±1.5% for the rosiglitazone-, GW9662-group and sham-groups respectively.

IR rats show higher MMR uptake in the infarct zone compared to shams for all time points imaged, with the highest difference at day5 (rosiglitazone 1.14±0.13%; GW9662 1.11±0.67% and sham 0.49±0.13%). Correlation was significant between perfusion and MMR presence, r=-.50, p=.0018. PPARgamma-activator rosiglitazone did not change the M2 macrophage recruitment after IR injury compared to the PPARgamma-inhibitor GW9662 in our experiment.

Conclusions: As in our previous experiments, we did show recruitment of M2-macrophages in the infarcted area. However, at this point, we were not able to demonstrate using SPECT/CT imaging a different impact of PPAR-gamma activation and inhibition on the recruitment of M2-macrophages after myocardial ischemia/reperfusion injury. For further analysis, animal groups will be expended, correlation between perfusion and MMR presence will be followed up and dose dependent effects will be examined.

References: 1. Bouhlel, M. A. et al. Cell metabolism 6, 137–43 (2007). 2. Anzai T. Circulation Journal 77(3), 580-7 (2013). 3. Nahrendorf, M. et al. The Journal of experimental medicine 204, 3037–47 (2007). 4. Harel-Adar, T. et al. PNAS 108, 1827–32 (2011).
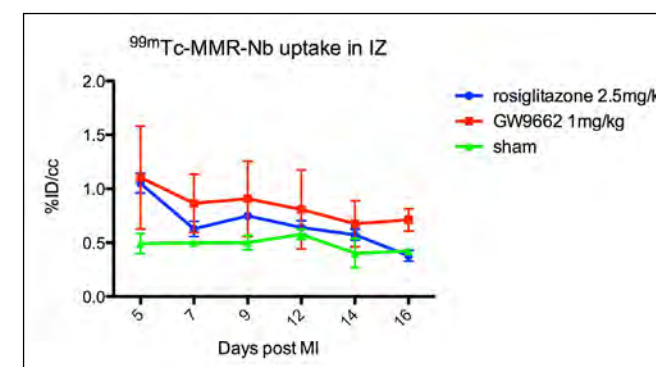
99mTc-MMR-Nb uptake: longitudinal data 99mTc-MMR-Nb uptake in infarct zone, mean and SEM depicted for each treatment group